AD-A135 793   RADIATIVE COLLISIONAL LASER FEASIBILITY DEMONSTRATION   1/1
(U) WESTERN RESEARCH CORP SAN DIEGO CA K Y TANG ET AL.
07 DEC 83 WRC-713-R N00014-82-C-0071

UNCLASSIFIED   F/G 20/5   NL

END
DATE
FILMED
1 84
DTIC

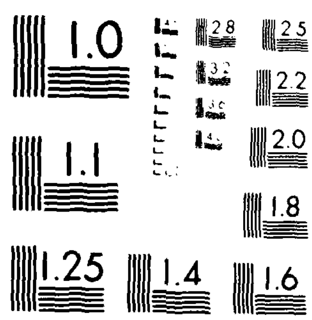

MICROCOPY RESOLUTION TEST CHART

12

AD-A135793

Copy No. 13

WRC-713-R

7 December 1983

FINAL REPORT FOR

RADIATIVE COLLISIONAL LASER FEASIBILITY DEMONSTRATION

CONTRACT NUMBER: N00014-82-C-0071

CONTRACT PERIOD: 16 NOVEMBER 1981 - 15 FEBRUARY 1983

Prepared for:

DEFENSE ADVANCED RESEARCH PROJECTS AGENCY
1400 Wilson Boulevard
Arlington, Virginia 22209

OFFICE OF NAVAL RESEARCH
800 North Quincy Avenue
Arlington, Virginia 22217

Prepared by:

WESTERN RESEARCH CORPORATION
8616 Commerce Avenue
San Diego, California 92121

UNCLASSIFIED

SECURITY CLASSIFICATION OF THIS PAGE (When Data Entered)

REPORT DOCUMENTATION PAGE		READ INSTRUCTIONS BEFORE COMPLETING FORM
1. REPORT NUMBER WRC-713-R	2. GOVT ACCESSION NO. A135793	3. RECIPIENT'S CATALOG NUMBER
4. TITLE (and Subtitle) FINAL REPORT FOR RADIATIVE COLLISIONAL LASER FEASIBILITY DEMONSTRATION		5. TYPE OF REPORT & PERIOD COVERED FINAL REPORT 16 Nov 1981 - 15 Feb 1983
		6. PERFORMING ORG. REPORT NUMBER WRC-713-R
7. AUTHOR(s) K. Y. Tang, L. W. Downes (ARGO), R. A. Tilton, S. D. Marcum (ARGO), W. E. Wells, Jr. (Assoc.Prof., Miami Univ.)		8. CONTRACT OR GRANT NUMBER(s) N00014-82-C-0071
9. PERFORMING ORGANIZATION NAME AND ADDRESS WESTERN RESEARCH CORPORATION 8616 Commerce Avenue San Diego, CA 92121		10. PROGRAM ELEMENT, PROJECT, TASK AREA & WORK UNIT NUMBERS DARPA Order Number 4367 Dated 14 Aug 1981
11. CONTROLLING OFFICE NAME AND ADDRESS DEFENSE ADVANCED RESEARCH PROJECT AGENCY 1400 Wilson Boulevard Arlington, VA 22209		12. REPORT DATE 7 Dec 1983
		13. NUMBER OF PAGES 54
14. MONITORING AGENCY NAME & ADDRESS (if different from Controlling Office) OFFICE OF NAVAL RESEARCH 800 North Quincy Avenue Arlington, VA 22217		15. SECURITY CLASS. (of this report) Unclassified
		15a. DECLASSIFICATION/DOWNGRADING SCHEDULE

16. DISTRIBUTION STATEMENT (of this Report)

"APPROVED FOR PUBLIC RELEASE; DISTRIBUTION UNLIMITED. REPRODUCTION IN WHOLE OR IN PART IS PERMITTED FOR ANY PURPOSE OF THE UNITED STATES GOVERNMENT."

17. DISTRIBUTION STATEMENT (of the abstract entered in Block 20, if different from Report)

18. SUPPLEMENTARY NOTES

19. KEY WORDS (Continue on reverse side if necessary and identify by block number)

Collisional Radiative Process
Metastable State
Excimer Kinetics
Electron Beam Excitation

20. ABSTRACT (Continue on reverse side if necessary and identify by block number)

Collisional radiative process between metastable state He and ground state N_2 has investigated through two separate experiments: i) Gain/absorption in electron-beam excited He/N_2 gas mixtures, and ii) change of He metastable density in the presence of external photon flux. No net gain was observed in He/N_2 system as it was presumably overwhelmed by the background absorption. However, the preliminary results of our He metastable density measurement gives strong evidence for existence of collisional radiative process.

DD FORM 1473, 1 JAN 73 EDITION OF 1 NOV 65 IS OBSOLETE

S/N 0102-LF-014-6601

UNCLASSIFIED

SECURITY CLASSIFICATION OF THIS PAGE (When Data Entered)

Copy No. 18

WRC-713-R
7 December 1983

FINAL REPORT FOR
RADIATIVE COLLISIONAL LASER FEASIBILITY DEMONSTRATION

CONTRACT NUMBER: N00014-82-C-0071

CONTRACT PERIOD: 16 NOVEMBER 1981 - 15 FEBRUARY 1983

Prepared for:

DEFENSE ADVANCED RESEARCH PROJECTS AGENCY
1400 Wilson Boulevard
Arlington, Virginia 22209

OFFICE OF NAVAL RESEARCH
800 North Quincy Avenue
Arlington, Virginia 22217

Prepared by:

WESTERN RESEARCH CORPORATION
8616 Commerce Avenue
San Diego, California 92121

TABLE OF CONTENTS

SECTION I

INTRODUCTION

Under Defense Advanced Research Projects Agency (DARPA) Contract N00014-82-C-0071, Western Research Corporation (WRC) and ARGO Research Corporation have jointly conducted two experiments to evaluate the laser amplifier performance via the collisional radiative process in He/N_2 system. The first experiment involved a series of measurements of gain/absorption in electron beam pumped He/N_2 gas mixtures, and the second experiment involved a measurement of change of He metastable density via collisional radiative process in the presence of external photon flux. The results of the experimental studies are summarized below, with a more detailed discussion of the results in Section 3. Analysis of the data has produced strong evidence for the proposed upper laser band pumping process, suggesting a very high probability of demonstrating absolute gain in the He/N_2 system.

Our gain/absorption measurements were made with He/N_2 mixtures in the wavelength region between 3530-3540 Å. Although absolute gain has not yet been observed, we have obtained absorption spectra with distinctive structure which follows closely the predicted collisional radiative transitions at 3532.6 and 3538.3 Å. Measurements conducted in pure helium show only a broadband and structureless absorption in the same region. We have not yet been able to completely explain the absorption, and believe that it may be due to an impurity.

Our second effort of testing the collisional radiative process, which was independent of gain, involved the measurement of depression of the He metastable density with an external photon flux. The relative He metastable density was monitored at a time ~500 ns after the electron beam was terminated. We have observed the metastable depression being ~30 percent at 3538 Å. This value agrees well with the predicted value, ~20 percent. No change in He metastable density was observed when the photon flux was not tuned to the wavelengths corresponding to the collisional radiative transitions. Combining the absorption data with the metastable depression results, we conclude that we have, for the first time, obtained evidence to show the existence of the collisional radiative process.

SECTION 2

THEORETICAL APPROACH

2.1 GENERAL CONSIDERATION

In 1972, Gudzenko and Yakovlenko[1] described a process whereby a photon induces collision and energy transfer between two different atomic of molecular species. The predicted reaction is

$$X(1) + Y(2) + \hbar\omega \rightarrow X(2) + Y(1)$$

where 1 and 2 refer to different energy levels of X and Y, the higher number indicating the higher energy. The process can be described quantum mechanically in terms of an intermediate state $X(1) + Y^V$ where Y^V represents a virtual level of Y a distance away from a real state. The complete reaction is then

$$X(1) + Y(2) + \hbar\omega \rightarrow X(1) + Y^V \rightarrow X(2) + Y(1) \quad .$$

This reaction is depicted schematically in Figure 2-1. Species Y(2) absorbs a photon thereby creating the quasimolecule $X(1) + Y^{v}$ which is energy resonant with X(2) + Y(1). The quasimolecule dissociates producing the final state X(2) + Y(1). Alternately, one can view the process as the formation of a quasimolecule X(1)Y(2), the absorption of a photon by the quasimolecule to form $X(1)Y^{v}$, followed by dissociation of $X(1)Y^{v}$ into X(2) + Y(1). In either case, the calculation for small detuning energies yields a cross section which is a function of photon flux and, for large photon fluxes, is large compared to normal inelastic cross sections.

The production rate for the X(2) state is

$$\frac{d[X(2)]}{dt} = kp[Y(2)][X(1)] = \langle \sigma v \rangle [Y(2)][X(1)]$$

where [] indicates concentrations, k is the rate coefficient, p the photon flux, v the relative velocity of X and Y, and σ the equivalent of a two-body cross section. Written in this form, σ depends on the photon flux. Harris[2] has used a collisional model to derive an explicit expression of σ. He finds that for low photon flux, σ is directly proportional to the photon flux and inversely proportional to the square of the detuning energy $\delta\omega$. At high photon flux, the Stark shift becomes important, and the cross section is proportional to the two-thirds power of the ratio of the photon field strength to the detuning energy.

Harris,[2-4] and others,[5] have measured very high cross sections for these reactions. To date, the highest reported cross section is 8×10^{-13} cm^2. This is three orders of magnitude larger than cross section for gas kinetic reactions. Such huge cross sections can control the energy pathways in the plasma. Consequently, radiative collisions have been suggested as mechanisms for producing population inversions in laser media.[4-6] Most of these schemes use the combined energy of the excited Y(2) and the photon to produce lasing

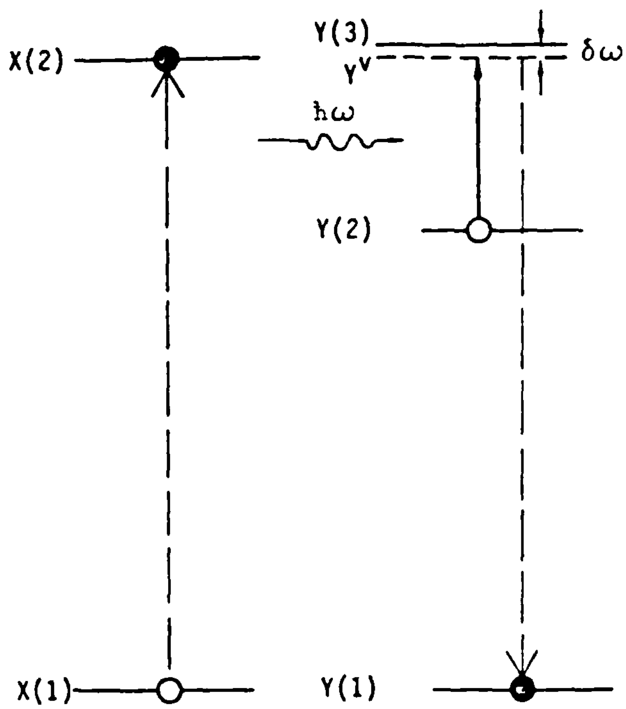

Figure 2-1. Radiative collision. The system begins (open circles) with Y in the state Y(2), X in the state X(1). Y absorbs a photon taking it to a virtual state from Y(3). The virtual state Y^V is energy resonant with X(2) to which it transfers its excitation energy. The final state of the system is indicated by solid circles.

from X(2) at short wavelengths. Hence they require one photon (visible or infrared) for radiative collisional photon (hard uv) produced. In the scheme described below the photon produced by the radiative collision have the same frequency as the photons required to stimulate the collision.

2.2 LASER PROCESS

The radiative collision can be couched in the form of stimulated absorption. The production rate for the final state X(2) is then

$$\frac{d[X(2)]}{dt} = B_{12}\rho[X(1)]$$

where $B_{12} = k[Y(2)]$ is the equivalent Einstein B coefficient. Now consider the stimulated emission process

$$\hbar\omega + X(2) + Y(1) \rightarrow X(1) + Y(2) + 2\,\hbar\omega \ .$$

The corresponding B coefficient is

$$B_{21} = \frac{g_{X(1)}g_{Y(2)}}{g_{X(2)}g_{Y(1)}} B_{12}$$

where the g's are the statistical weight for the atomic or molecular levels which comprise the upper and lower laser states. The photon production rate is the difference between the stimulated emission and absorption processes. So

$$\frac{d\rho}{dz} = \hbar\omega \ \frac{d[X(1)]}{dt} = k\rho \left\{ \begin{array}{l} g_{X(2)}g_{Y(1)}[X(2)][Y(1)] \\ -g_{X(1)}g_{Y(2)}[X(1)][Y(2)] \end{array} \right\}.$$

The corresponding gain is

$$\gamma = \frac{1}{p}\frac{dp}{dt} = \hbar\omega k \left\{ \begin{array}{l} g_{X(2)}g_{X(1)}[X(2)][Y(1)] \\ - g_{X(1)}g_{Y(2)}[X(1)][Y(2)] \end{array} \right\}$$

The gain is proportional to the difference between the product of the densities of states for X(2) and Y(1), and the product of the densities of states for X(1) and Y(2). This fact allows new mechanisms for producing population inversions. For example, energy storage in the upper laser level might occur in X(2), whereas destruction of the lower laser level might occur owing the auto-ionization of Y(2). Just such a mechanism is the basis for the [illegible]dicted radiative collisional laser in He/N_2.

2.3 RADIATIVE COLLISIONAL LASER IN He/N_2

Figure 2-2 depicts the relevant levels in the energy level diagrams of He and N_2. In the predicted radiative collisional laser, Wells and coworkers make the correspondence

$$X(1) \rightarrow He(1^{-1}S) \qquad Y(1) \rightarrow N_2(X)$$

$$X(2) \rightarrow He(2^3S) \qquad Y(2) \rightarrow N_2^{\star}(X,v3,4)$$

$$Y(3) \rightarrow N_2^{\star}(B,v=4,5)$$

where $N_2^{\star}(X,v)$ is an $N_2^{+}(X,v)$ ionic core with a Rydberg electron near the ionization limit. Similarly, $N_2^{\star}(B,v+1)$ is an $N_2^{\star}(B,v+1)$ ionic core with a Rydberg electron. The stimulated process is then

$$He(2^3S) + N_2(X) + \hbar\omega \rightarrow He(1^{-1}S) + N_2^{\star}(X,v) + 2\,\hbar\omega \quad .$$

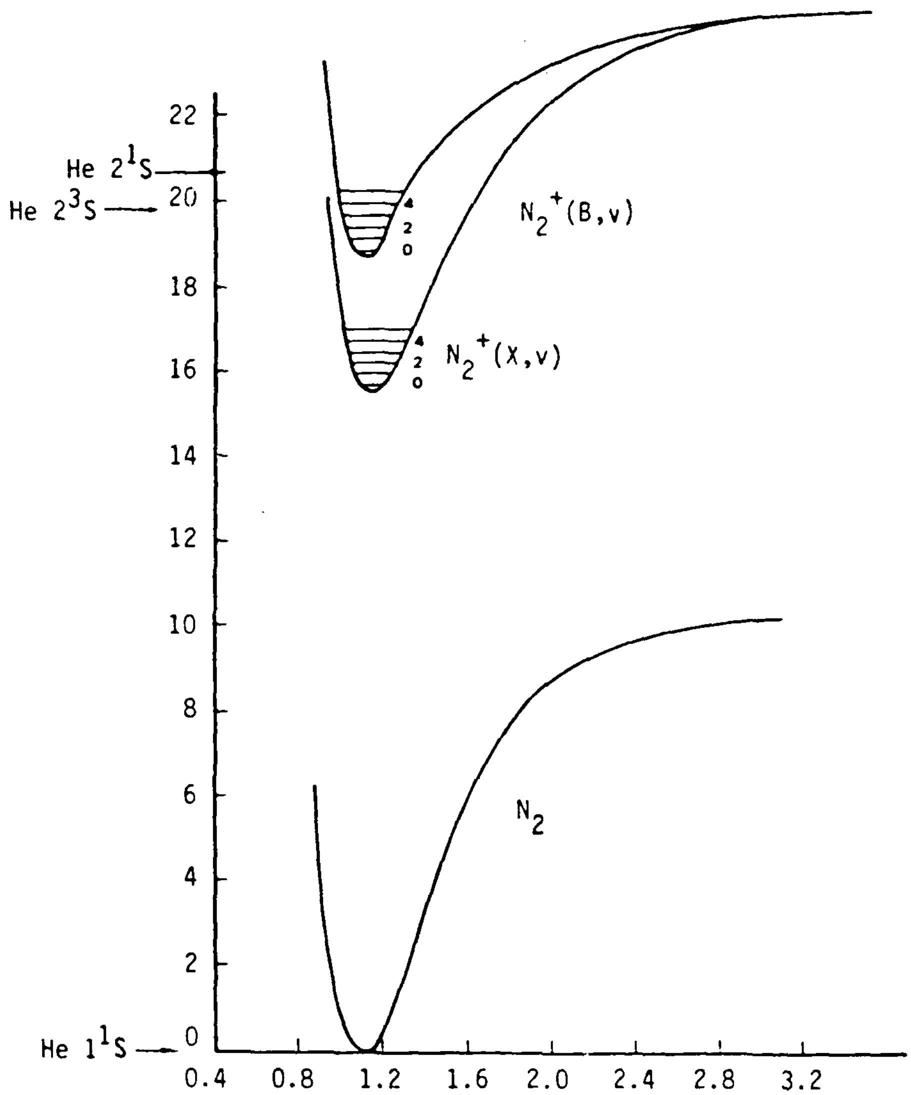

Figure 2-2. He/N_2 energy level diagram. The diagram is abbreviated for clarity.

It is assumed that since the Rydberg electron is far from the ionic core, it does not participate in the radiative transition so the transition wavelength are essentially those of the equivalent ionic transition. Figure 2-3 gives the wavelengths and Einstein coefficients for the $N_2^+(B,v') \rightarrow N_2^+(X,v'')$ transitions. Upper levels with $v \leqslant 3$ fall below the $He(2^3S)$ energy level, so are not candidates for radiative collisions. Consequently, the best candidates appear to be the $4 \rightarrow 3$ transition at 3538 Å and the $5 \rightarrow 4$ transition at 3532 Å.

Wells[6] uses the expression derived by Harris[2,3] to determine the cross section. Since the Rydberg state is effectively in the Saha continuum, the detuning energy is taken to be a convolution of the linewidths of the excited states and the bandwidth of the incoming photon flux field. He estimates this value to be 2 cm^{-1}. Figure 2-4 shows the resulting cross section in the low and high photon flux regimes. Wells performs a model calculation for one percent N_2 in 1 atm of He for power depositions from 20 W/cm^2 to 20 MW/cm^2. Since the $N_2^*(X,v)$ state autoionizes[7] in about 10^{-10} s by giving up one quantum of vibrational energy to the Rydberg electron, the ground state density of the laser is negligible. The decrease in predicted steady state gain shown in Figure 2-5 with increasing photon flux is due to the high destruction rate for the metastable density which accompanies increasing cross section. This effect is shown more clearly in Figure 2-6 which depicts the steady state metastable density as a function of photon flux. The energy extraction efficiency is depicted in Figure 2-7. At low photon flux the efficiency is poor so the system makes an inefficient laser oscillator. On the other hand, at high photon flux fields, the efficiency approaches the quantum efficiency and saturates near 15 percent. This efficiency is quite acceptable for amplification at high power.

Lower Vibrational Level

Upper Vibrational Level	0	1	2	3	4	5
0	9.64 3914.4	3.48 4278.	.775 4709.	.136 5228.	.205 5864.	.283
1	4.87 3582.	3.08 3884.3	3.87 4236.	1.53 4652.	.392 5149.	.078 5653.
2	.757 3308.	6.36 3564.	.574 3857.9	3.03 4199.	1.94 4560.	.68 5077.
3	.028 3078.	1.64 3299.	6.24 3549.	.003 3835.4	1.98 4167.	2.00 4554.
4		.062 3076.	2.35 3293.	5.55 3538.	.154 3818.1	1.14 4140.
5			.072	2.78 3291.	4.83 3532.	.431 3806.8

Figure 2-3. Einstein coefficients (in units of 10^{+6}S) and wavelengths (in angstroms) for the first negative system of nitrogen.

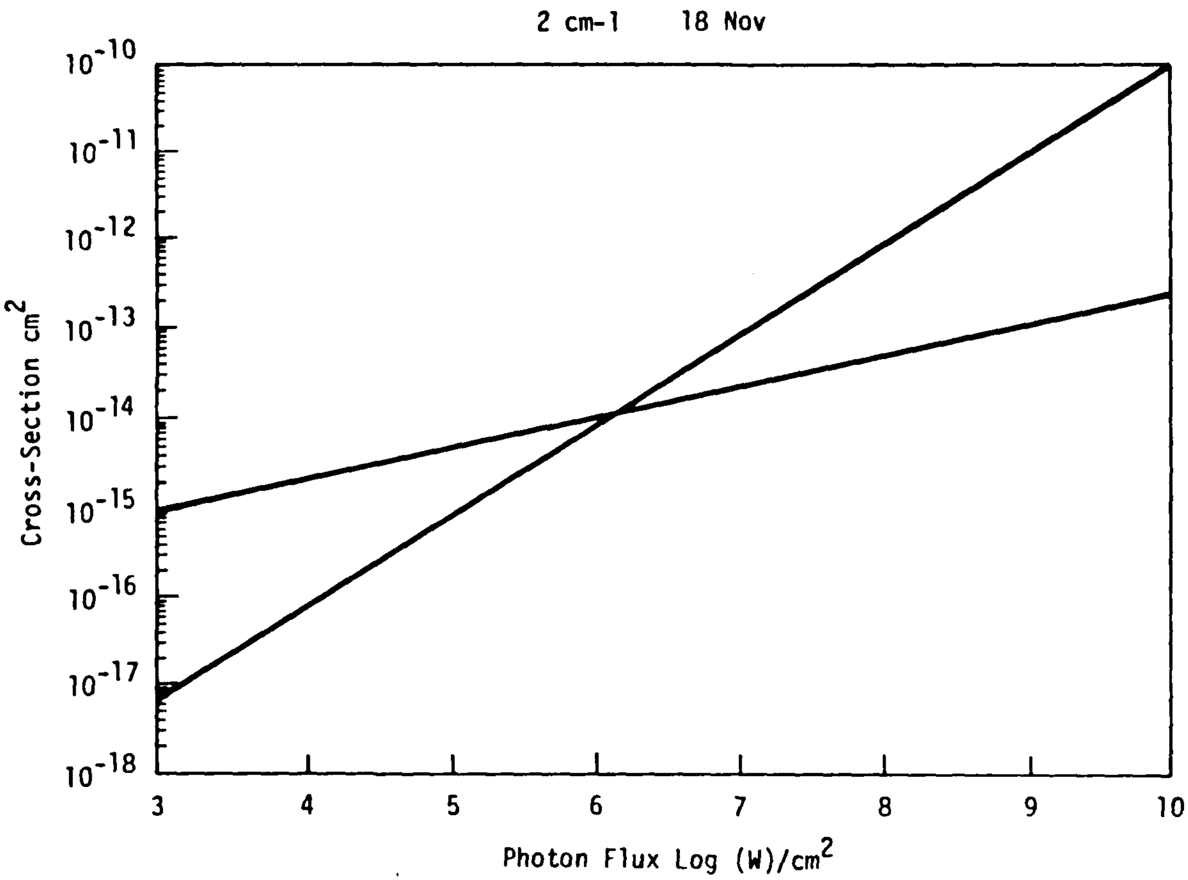

Figure 2-4. Cross Section. Theoretical radiative collisional cross section from model calculation in He/N_2 system.

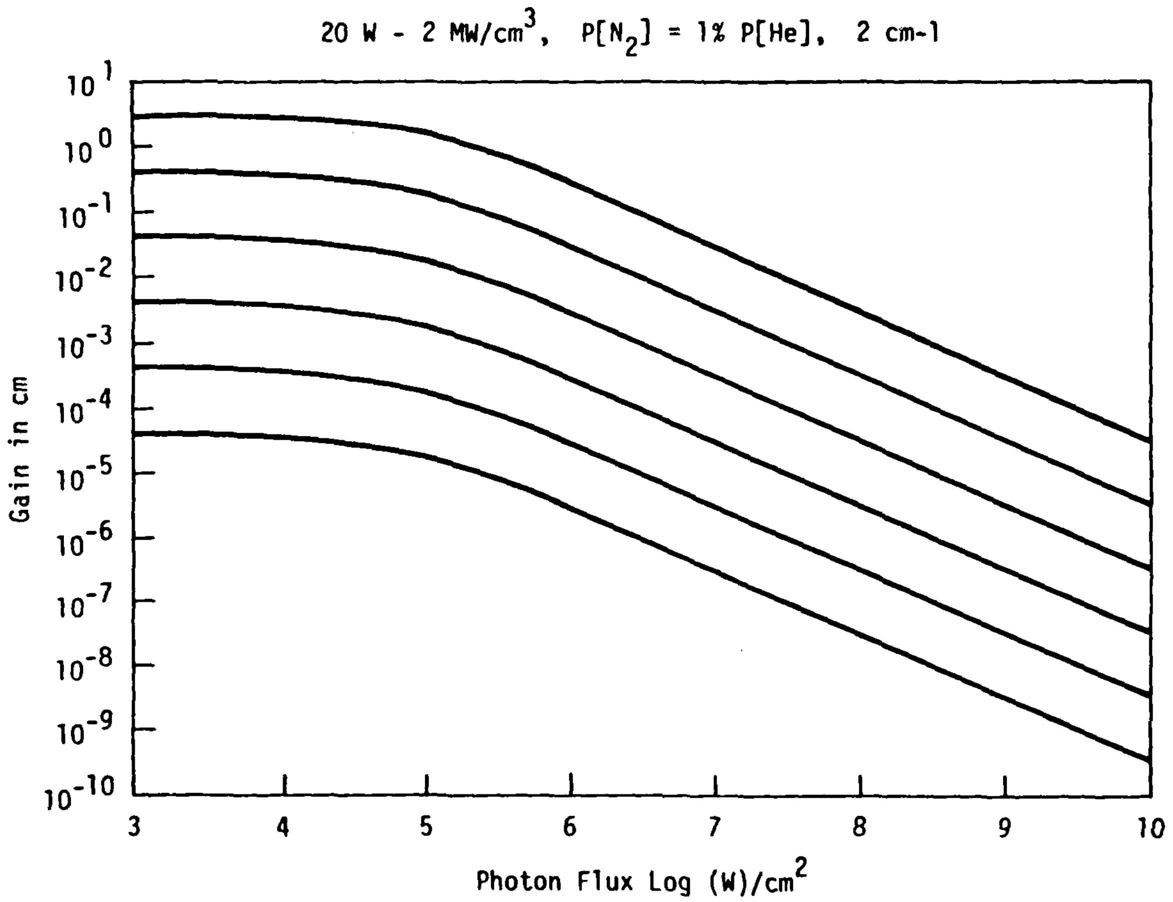

Figure 2-5. Gain. Predicted gain in the He/N_2 system for power depositions from 20 W/cm^3 to 2 MW/cm^3 (upper curve).

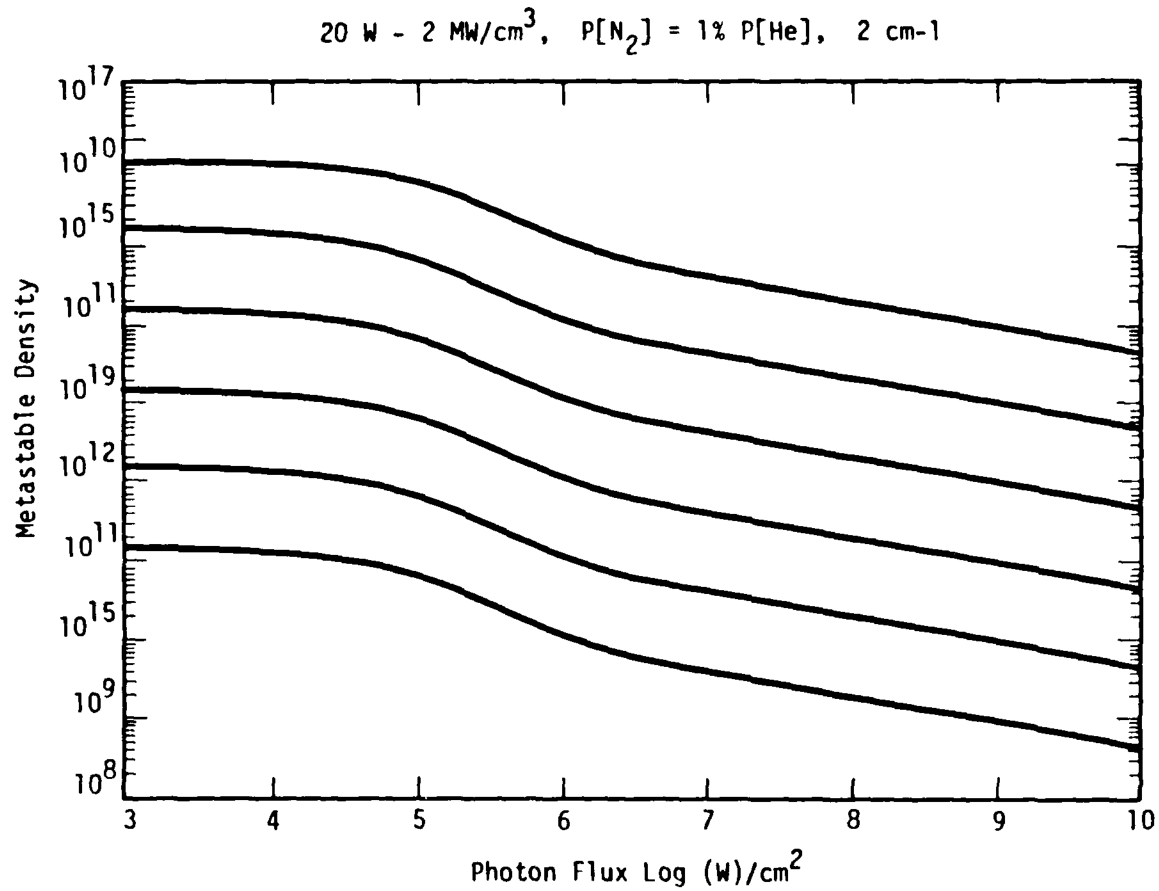

Figure 2-6. Metastable Density. Predicted helium metastable density for He/N_2 system for power depositions from 20 W/cm^3 to 2 MW/cm^3.

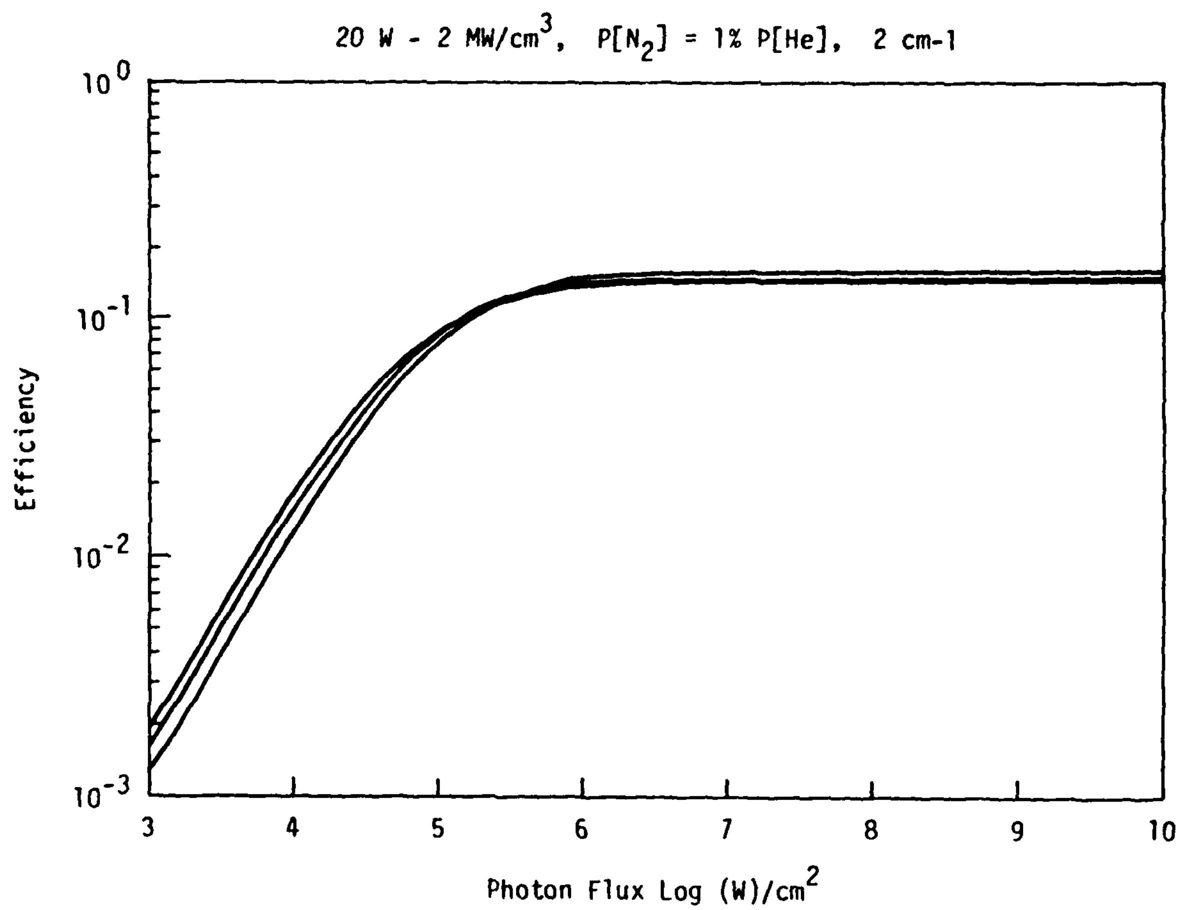

Figure 2-7. Efficiency. Predicted efficiencies for the He/N_2 system at power depositions from 20 W/cm^3 to 2 MW/cm^3.

SECTION 3

EXPERIMENTAL RESULTS

3.1 FLOWING AFTERGLOW

We have conducted a flowing afterglow experiment in which we monitored the reaction between N_2 and He metastable via fluorescence emission. Emission at 3532 and 3538 Å has been detected. A portion of the emission spectrum is given in Figure 3-1. It was noted that in the afterglow the He(2'S) concentrations were not sufficient to explain the observed intensities at 3532 and 3538 Å. The lower energy $He(2^3S)$ was present in much larger quantities but does not have sufficient energy to produce $N_2^+(B,5)$ or $N_2^+(B,4)$ states necessary to obtain these transitions in the ion. On the other hand, the reaction

$$He(2^3S) + N_2 \rightarrow He(1^{-1}S) + N_2^*(B,5 \text{ or } 4) \rightarrow He(1^{-1}S)$$

$$+ N_2^*(X,4 \text{ or } 3) + \hbar\omega$$

is energetically possible since the presence of the Rydberg electron lowers the energy of N_2 final product. The emission at 3532 Å and 3538 Å is taken as evidence for this reaction (which is both the reverse of the photon induced collision, and the spontaneous process on which the stimulated radiative collision is based). One can determine the cross sections for the reactions from the ratios of their emission strengths to the N_2 emission at 3914 Å. The cross section obtained in this way is about a factor two higher than the predicted cross section. Emission at 3538 Å and 3532 Å has also been observed in the stationary afterglow of electron beam pumped systems where

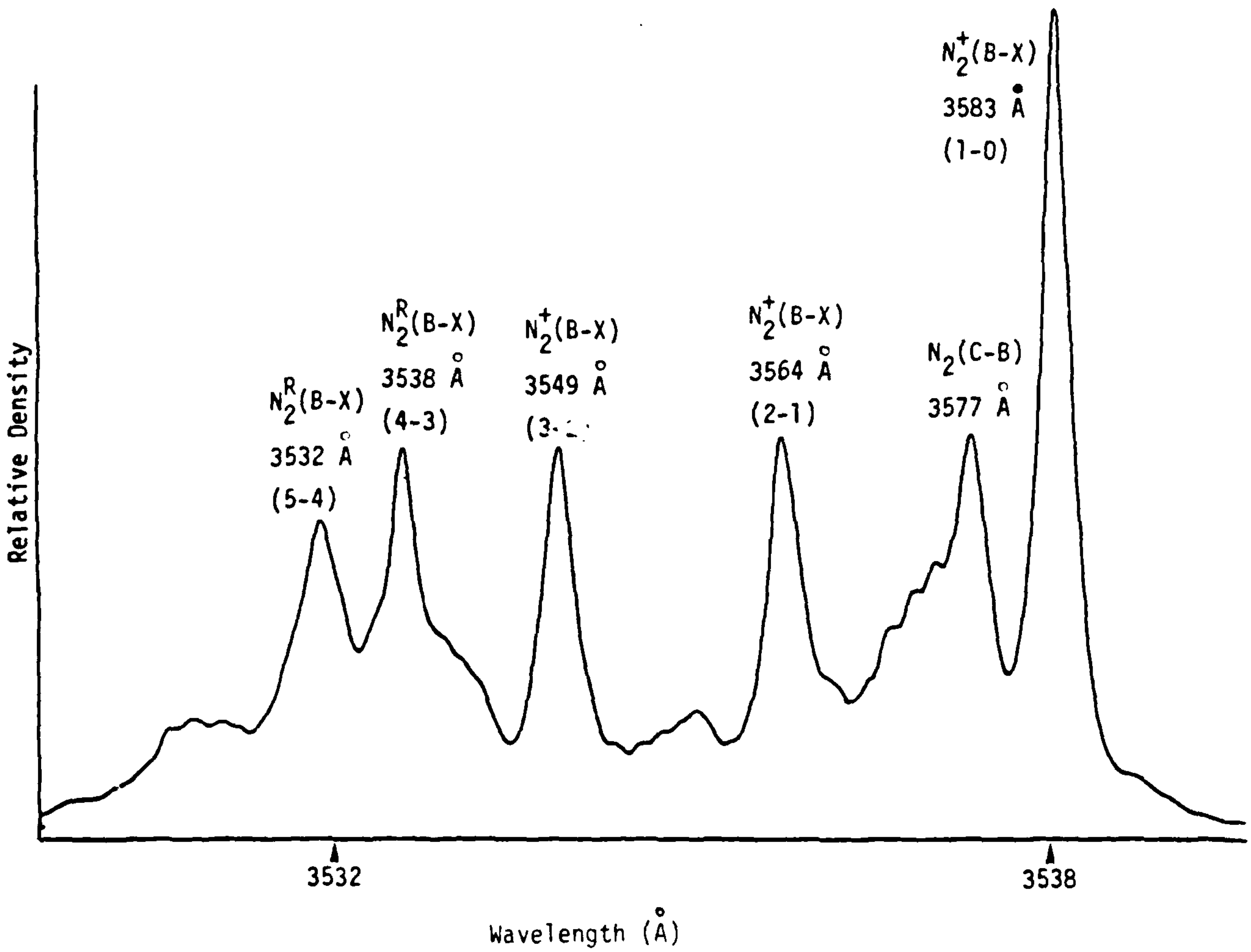

Figure 3-1. Portion of the fluorescence spectrum taken in the region where N_2 was mixed with He metastable generated by microwave discharge in the flowing afterglow experiment.

only He(2^3S) is present.[9] The cross sections obtained in this work agree very well with those obtained in the flowing afterglow experiments.

3.2 GAIN MEASUREMENT

The first experiment of evaluating the collisional radiative process was devised to show the gain in electron beam pumped He/N_2 system. A series of measurements were made with different gas mixtures. Only absorption was observed. However, structures which appear in the absorption spectra follow closely the predicted collisional radiative transitions, suggesting the existence of gain the He/N_2 system. In the following, we shall first briefly describe the experimental set-up used for the gain/absorption. We will then present the results and discuss the implications.

A standard set-up for the gain measurement is shown in Figure 3-2. This same setup was later adopted for the He metastable depression measurement with only a slight modification. Briefly, it consists of a probe laser and an electron beam pumped He/N_2 laser amplifier. The laser was a flashlamp pumped dye laser and was operated at near 710 nm. An angle-tuned frequency doubler was used to produce the second harmonic in the region between 353-354 nm. Although much effort has been spent, we were unable to obtain a good quality beam in the ultraviolet, nor were we able to exceed 100 kW/cm^2 in power density. A quartz prism was used to separate the fundamental from second harmonic frequencies so that only the UV part of the laser signal was utilized in the entire optical path. A thin quartz disc was used as beam splitter to provide a reference signal to a photodiode before the laser beam entered the amplifier

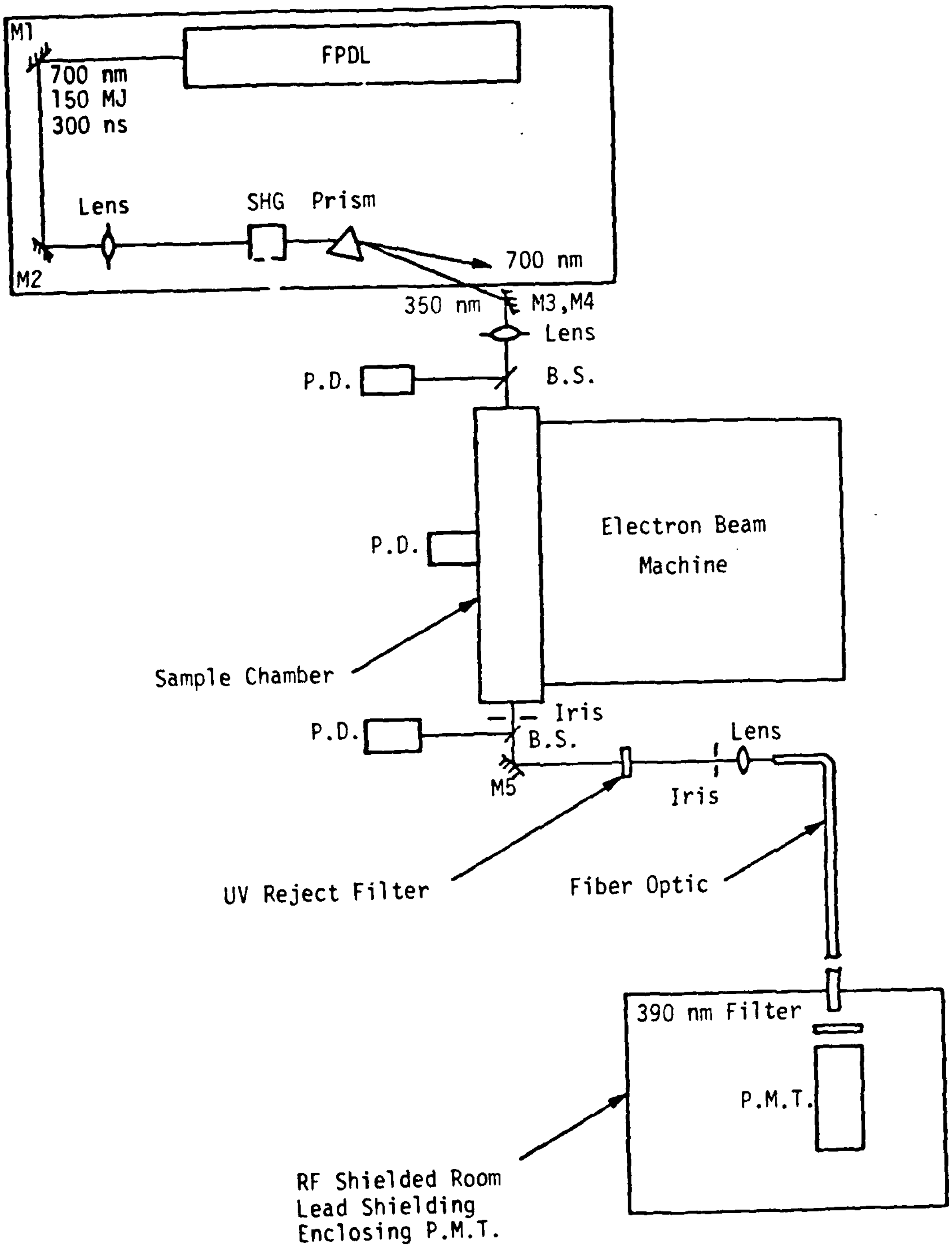

Figure 3-2. Experimental apparatus for gain/absorption and metastable depression measurement.

region. The amplifier was pumped by an electron beam machine with the following characteristics:

$$V = 350 \text{ kV}$$

$$J \cong 10 \text{ A/cm}^2$$

$$\text{Area} = 10 \times 120 \text{ cm}^2$$

$$\Delta t \leqslant 1 \ \mu s$$

After traversing the amplifier, the laser pulse was again split to another photodiode for gain/loss signal. Finally, a third photodiode was used to monitor a reference so that any variation, which might occur during the experiment, could be easily observed.

Gain or loss was determined by observing the ratio of the two photodiode signals with the dye laser fired during the electron beam excitation and comparing to the same ratio in the absence of electron beam. The ratio of these two ratios provided the ratio of I/I_0, the output intensity to the input intensity. The reproducibility was found to be no more than 10 percent.

In Figures 3-3 and 3-4, we present the results for the gain measurement with two different gas mixtures. The data point in each figure represents an average value from at least two measurements. The uncertainty of the measurement is indicated by the error bar shown in Figure 3-3.

From Figures 3-3 and 3-4, we first note that only absorption has been measured in our experiment. The absorption increased with the increase of He pressure. This could be due to the increase of the density of the absorber as the result of more energy deposition. We also note the general appearance of the absorption spectra which shows broad structures peaked at 3532.6 and 3538.3 Å, which correspond to the expected collisional

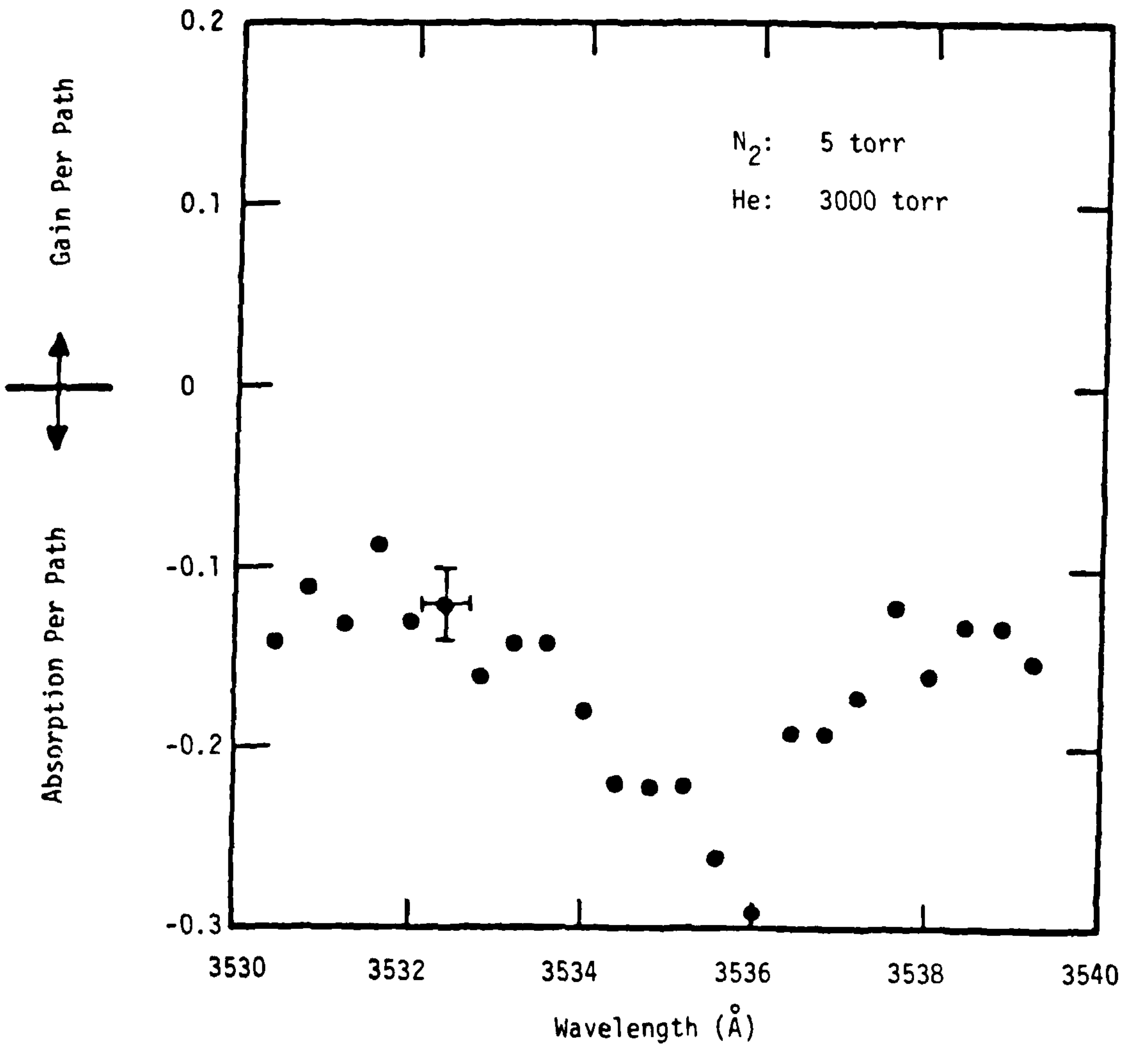

Figure 3-3. Gain/absorption measurements (Case 1).

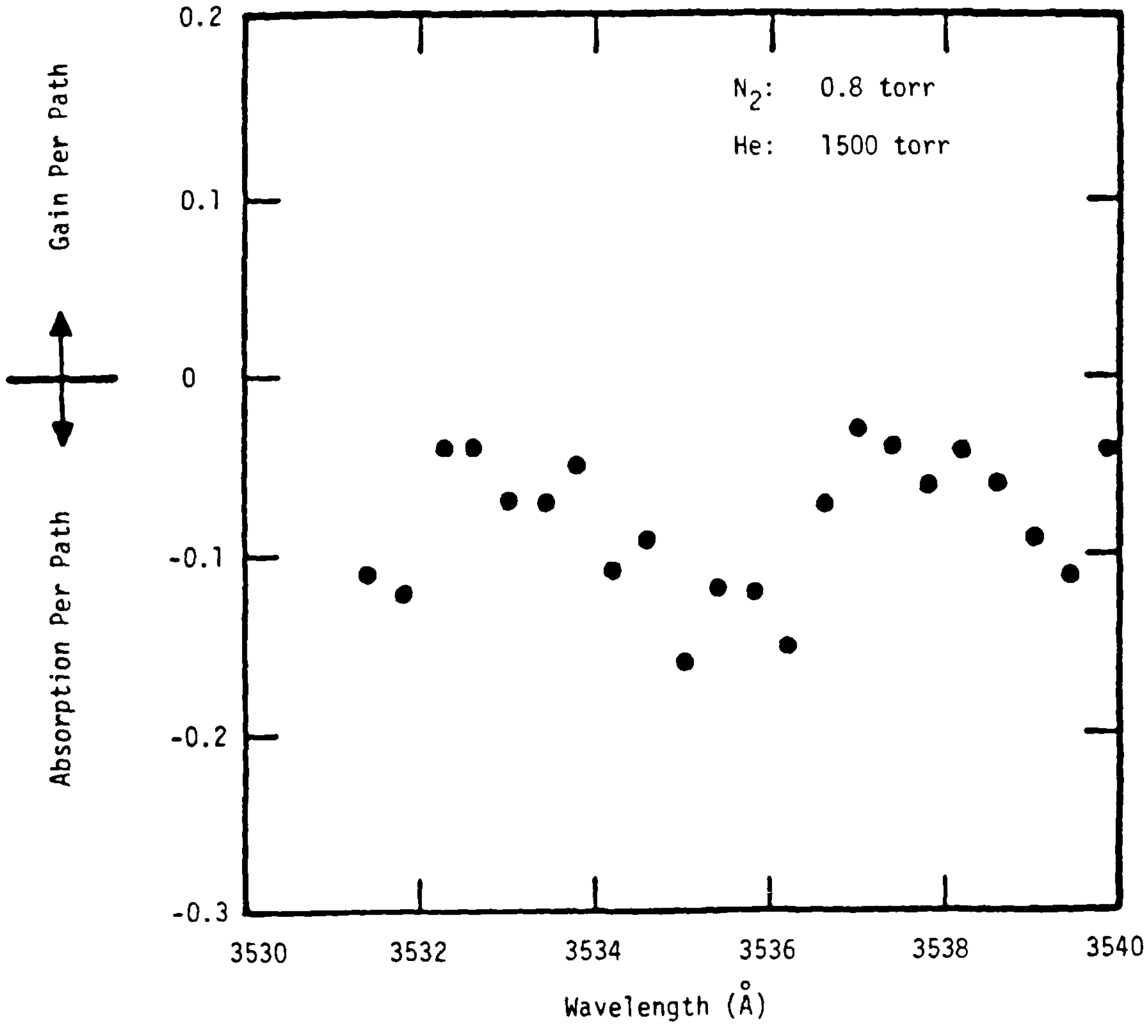

Figure 3-4. Gain/absorption measurements (Case 2).

radiative transitions. For a comparison, we show in Figure 3-5, a portion of spontaneous emission spectrum taken from the flowing afterglow experiment. Note the similarity in structure. The results in Figures 3-3 and 3-4 seem to suggest that the He/N_2 system may show a net gain at 3532.6 and 3538.2 A, and such gain was depressed by what appears to be an extraneous absorption which is dependent on overall pressure.

Results from the measurements made with pure helium is shown in Figure 3-6. Contrary to the He/N_2 spectra, we observe only a broad band, structureless absorption. Additional measurements indicate that such absorption is also pressure dependent.

No absorption was observed when measurement was made in the afterglow of the electron beam excitation. Thus, the absorber must be short-lived and exist only where excitation was maintained.

3.3 METASTABLE DEPRESSION

The gain structure provides some confidence that the collision process is indeed occurring. However, it is informative to observe the stimulation of the radiative collision directly.

The stimulated emission occurs from the reaction,

$$He(2^3S) + N_2(x) + \hbar\omega \rightarrow He(1^1s) + N_2^*(s,v) + 2\hbar\omega \quad .$$

In the afterglow of the e-beam excitation, there is an insignificant production of $He(2^3S)$ and a slow decay. When this time region is acted

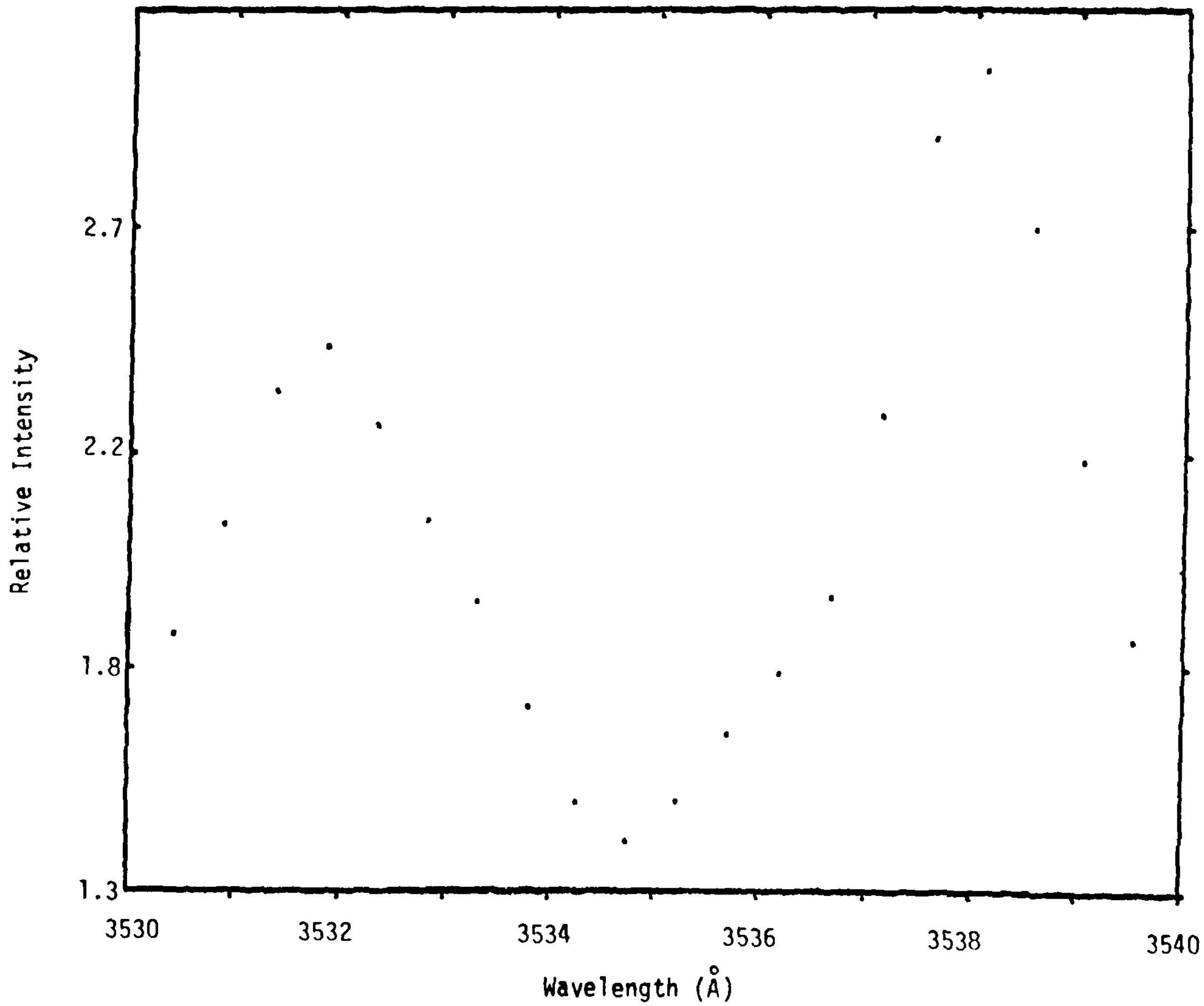

Figure 3-5. Flowing afterglow emission.

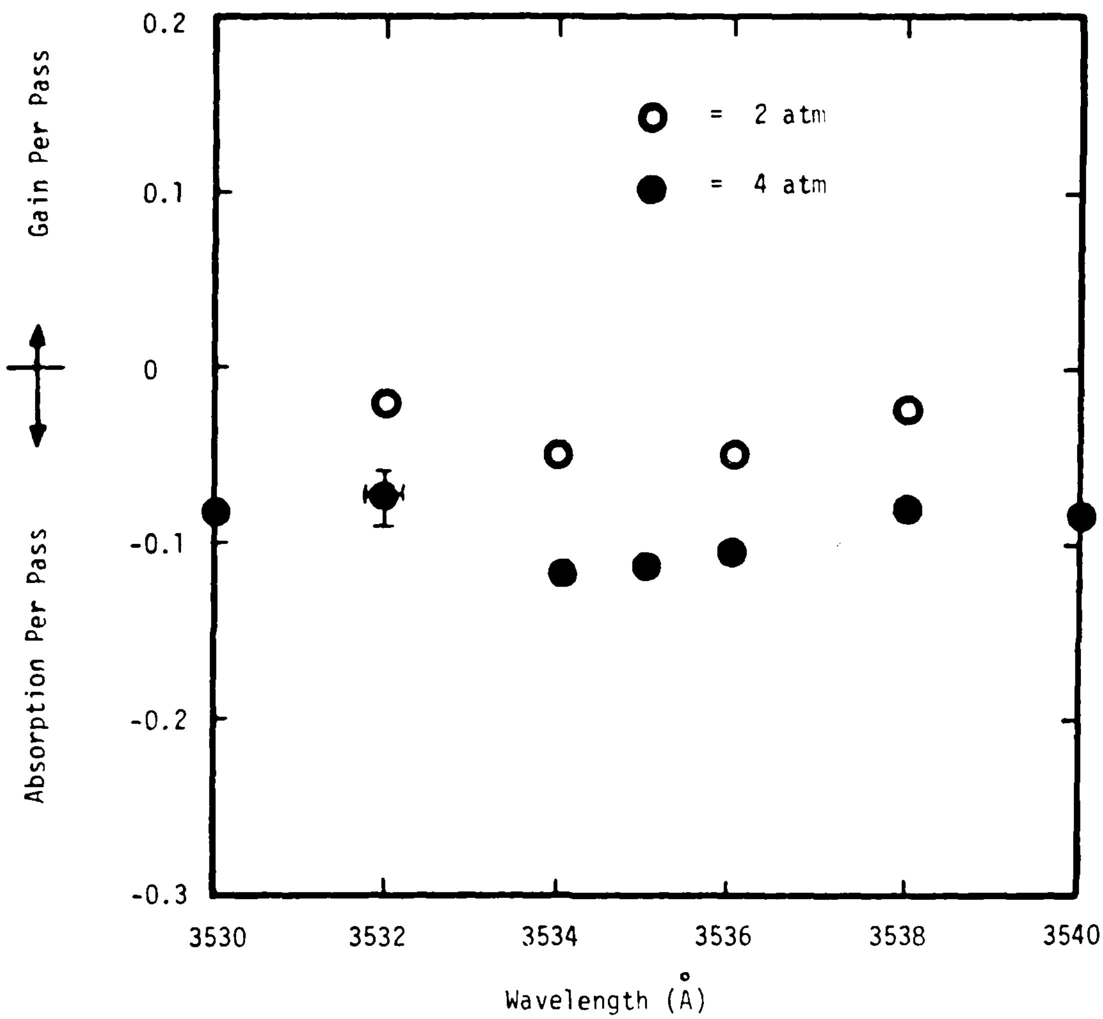

Figure 3-6. He Absorption.

on by a laser pulse, at the proper wavelength, then

$$\frac{dM}{dt} = - (\sigma_{RC} v) [M] [N_2], \text{ or}$$

$$\frac{dM}{M} = - (\sigma_{RC} v) [N_2] dt \quad .$$

This last equation represents a fractional change in the metastable density.

If the increase in the radiative collision cross section due to an impressed photon flux is larger than the normal decay process, then, we should see an increase in loss of metastables.

It has been well established that in the afterglow of a He/N_2 mixture, the $He(2^3S)$ density is controlled by the Penning reaction which produces emission at 3914 Å. As shown in the experimental set-up, Figure 3-2, an optical system which rejects the laser pulse at 3532 or 3538 Å and passes radiation at 3914 Å, which originates from the volume of the plasma affected by the laser pulse was used. The light signal is transmitted via a fiber optic cable to a shielded room for detection by a photomultiplier. In order to evaluate the resulting signal, it was digitized by a waveform digitizer with 50 ns resolution. This data was in turn stored by a microprocessor. The concentration of N_2 was chosen to be 0.05 percent in order to provide an observable afterglow. Using a 300 ns pulse at 100 kV/cm^2 and the cross section experimentally measured from spontaneous emission, in a 1 atm mixture, the fraction of change is

$$\frac{dM}{M} = (5 \times 10^{-16} \text{ cm}^2)(10^5 \text{ cm/s})(1.4 \times 10^{16} \text{ cm}^3)(3 \times 10^{-7} \text{ s}) = 0.2 \ .$$

Figure 3-7 shows the afterglow emission at 3914 Å with a detuned wavelength (3539 Å) laser pulse. No effect of the laser can be observed. The lifetime is approximately 400 ns which is comparable with the Penning reaction, and thus proportional to He[2^3S]. Figure 3-8 shows the same measurement; however, now the dye laser is tuned to 3538.3 A. Here a depression is obvious compared with the reference shot with the laser blocked (Figure 3-9). At late times, the metastable density is replenished by diffusion. The fractional change is about 30 percent.

Our data represent proof-of-principle and indicate gain should exist on this transition. However, the gain measurements indicate that absorption elsewhere in the system probably dominates in our experiments to date. No explanation for the observed absorption based on a pure He/N_2 system is apparent.

One point worth noting which possibly bears on the observed absorption was that the afterglow decay time changed with repeated shots with the same gas fill, indicating the possible existence of impurity species.

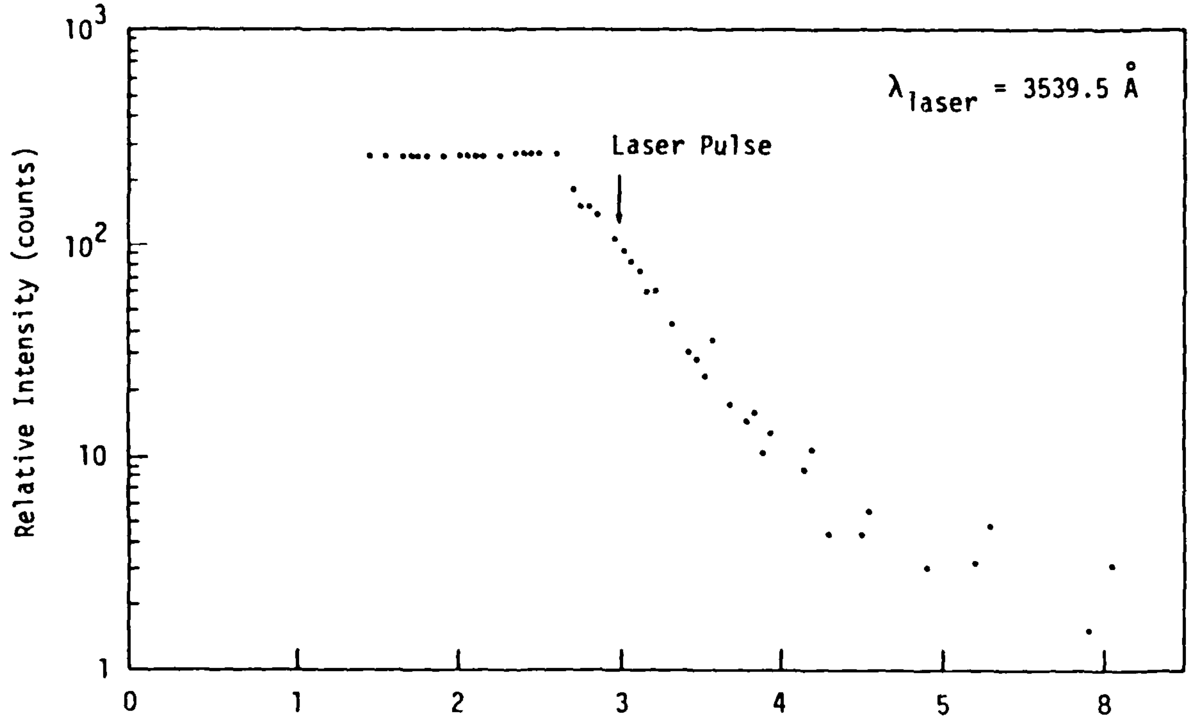

Figure 3-7. Afterglow emission at 3914 Å with detuned laser pulse

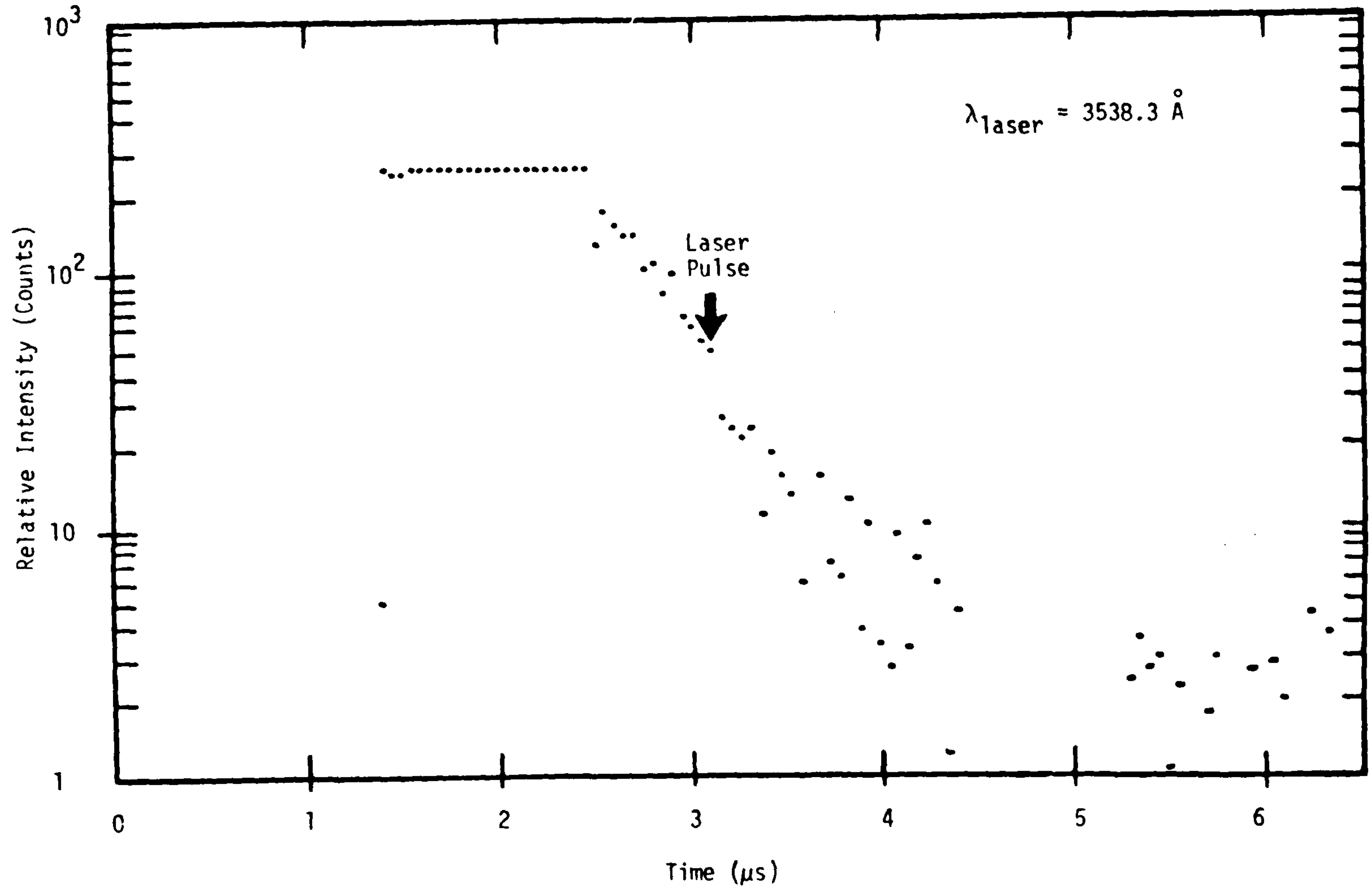

Figure 3-8. Afterglow emission at 3914 Å, showing depression due to laser pulse.

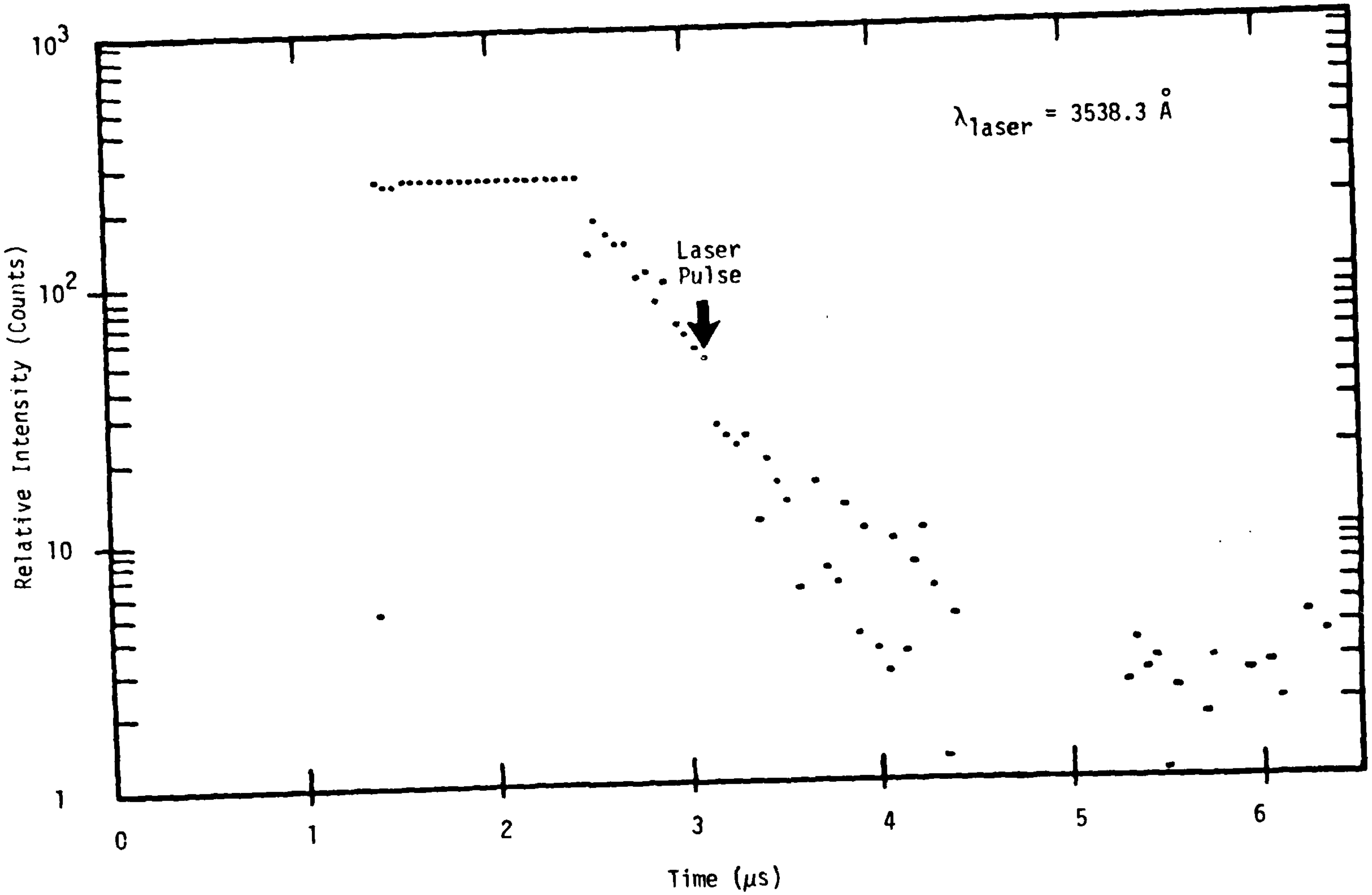

Figure 3-8. Afterglow emission at 3914 Å, showing depression due to laser pulse.

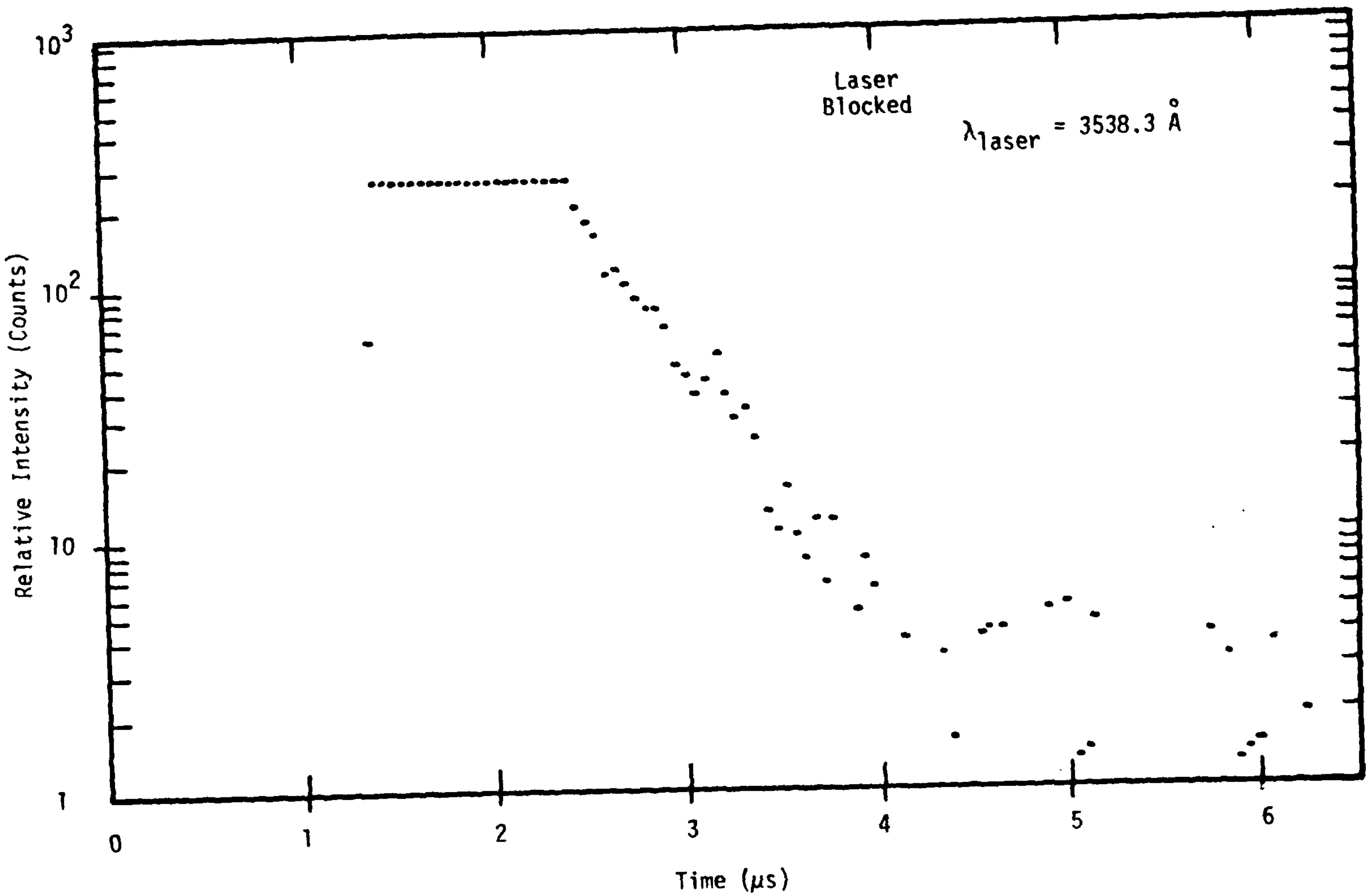

Figure 3-9. Afterglow emission at 3915 Å with laser blocked.

SECTION 4

CONCLUSION

Based on the gain/absorption data and the metastable He depression results presented in the previous section, we conclude that the proposed collisional radiative process does seem to exist in the He/N_2 system. Further investigation of such a process should include a more direct measurement of He metastable density (via absorption from the He metastable state) during the electron-beam excitation. Moreover, a detailed understanding of the background absorption in electron-beam pumped He/N_2 mixture is necessary in order to optimize the conditions for the experiment, whereby the net gain can be quantitatively determined.

SECTION 5

REFERENCES

1. L. I. Gudzenko and S. I. Yakovlenko, Sov. Phys. JETP 35, 877 (1972).

2. S. E. Harris, J. F. Young, W. R. Green, R. W. Falcone, J. Lukasik, J. C. White, J. R. Willison, M. D. Wright and G. A. Zdasiuk, "Laser Induced Collisional and Radiative Energy Transfer," Proceedings of Laser Spectroscopy IV (June 1979).

3. W. R. Green, M. D. Wright, J. Lukasik, J. F. Young and S. E. Harris, Opt. Letts. 4, 265 (1979).

4. S. E. Harris, Opt. Letts. 5 (1980).

5. J. C. White, Opt. Letts. 5, 199 (1980).

6. L. W. Downes, S. D. Marcum, R. A. Tilton and W. E. Wells, Opt. Letts. 7, 22 (1982), also see Appendix.

7. C. Duzy and R. S. Berry, J. of Chem. Phys. 64, 2431 (1976).

8. S. D. Marcum, private communication.

9. J. Goldhar and J. R. Murray, Opt. Letts. 1, 199 (1977).

10. J. Goldhar, W. R. Rapoport and J. R. Murray, J. of Q. Elect. QE-16, 235, (1980).

11. W. R. Rapoport, J. Goldhar and J. R. Murray, "Tuning and Extraction of XeCl," Lawrence Livermore Laboratory Internal Rpoert AL70-109 04060 (8 January 1980).

12. J. Goldhar, J. Dickie, L. P. Bradley and L. D. Pleasance, App. Phys. Letts. 31, 677 (1977).

APPENDIX I

MODEL CALCULATION

The experimental evidence for the absorber indicates that its density increases with pressure, and is very short lived (no absorption in the afterglow), with broad band absorption. The $He(2^3s)$ is long lived and, therefore, is eliminated as a candidate.

A model, described here, has been developed for the He/N_2 system. We have used this system to examine the variation of densities as a function of pressure. Results indicate that as the pressure increases, all species also increase. This makes all of the species candidates for the absorber, except for the $He(2^3s)$. However, He^+ and N_2^+ are not known to have broad band absorption. He_2^+ doesn't have a known broad band absorption but such absorption has been seen in Xe_2^+, Kr_2^+ and other rare gases and may be a candidate. Again, impurities are not considered in this model, but should follow the He_2^+ example.

The model was used with the N_2 concentration set to zero in order to evaluate the data. These results are shown in Table I. In increasing the pressure from 1 to 4 atm., the He_2^+ density changes from 3×10^{13} to 4.4×10^{13} cm^{-3}, which is far short of the factor of ~ 2.5 shown in the main text.

TABLE I*

Pressure	He^+	He_2^+	$He2^3s$
1 Atm.	4.5×10^{12}	3×10^{13}	6.3×10^{14}
4 Atm.	3.6×10^{12}	4.4×10^{14}	9.5×10^{14}

*Energy deposition = 2.5 KW/cm^3 per atmosphere of He.

Included herewith for completeness is also a set of plots of the ratio of He_2^+ to $He(2^3s)$ as a function of photon flux. In these plots, PHE refers to the He pressure in torr and PD to the power deposition in W/cm^3. It was realized that if the absorption or gain is tied to this ratio, then a ratio of less than 1.5×10^{-2} will be necessary for gain. An example species density plot with no photon flux for one of many combinations of He/N_2 examined is also include here.

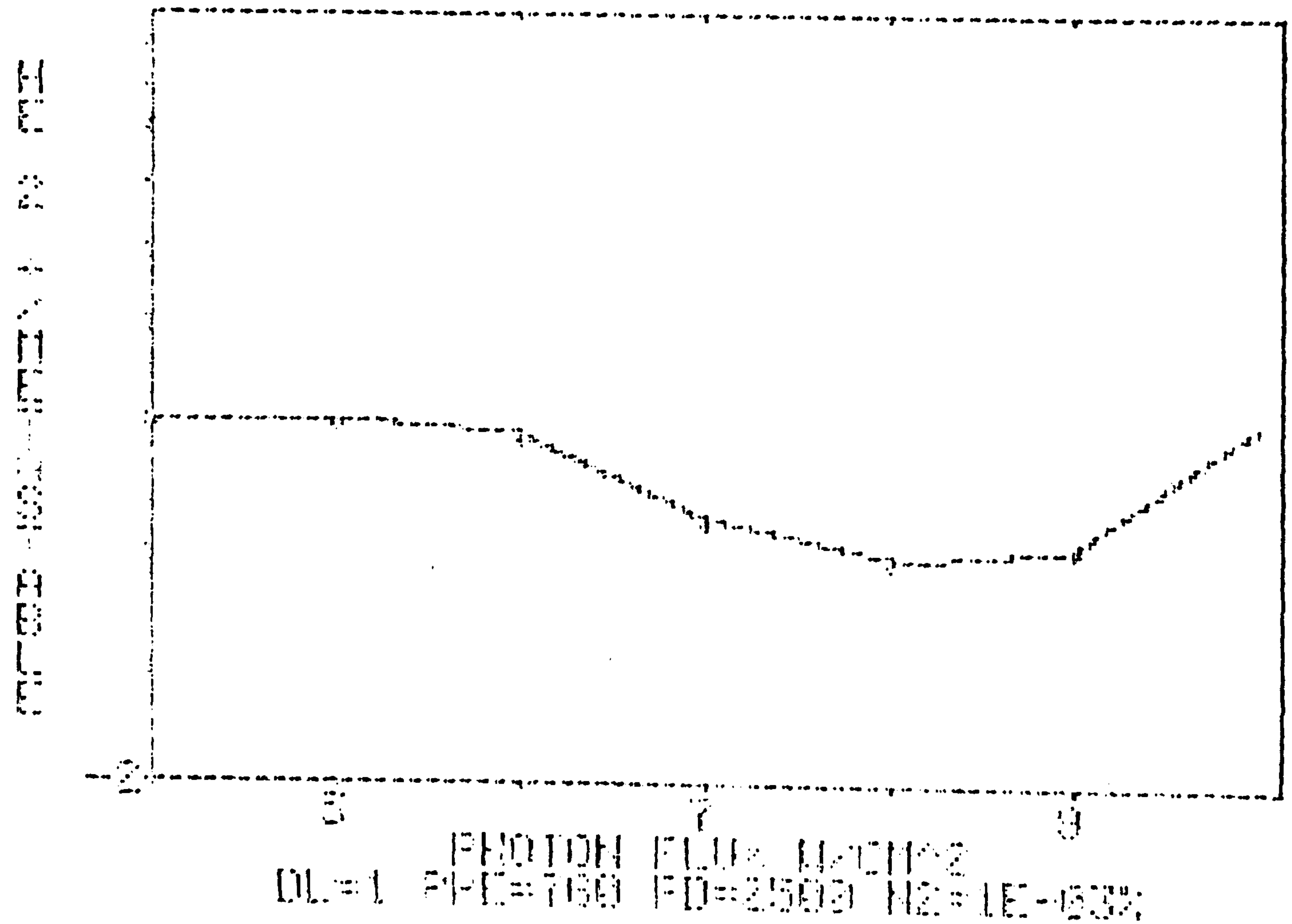
-2
5
7
9
PHOTON FLUX W/CM^2
DL=1 PHC=700 PD=2500 H2=1E-03%

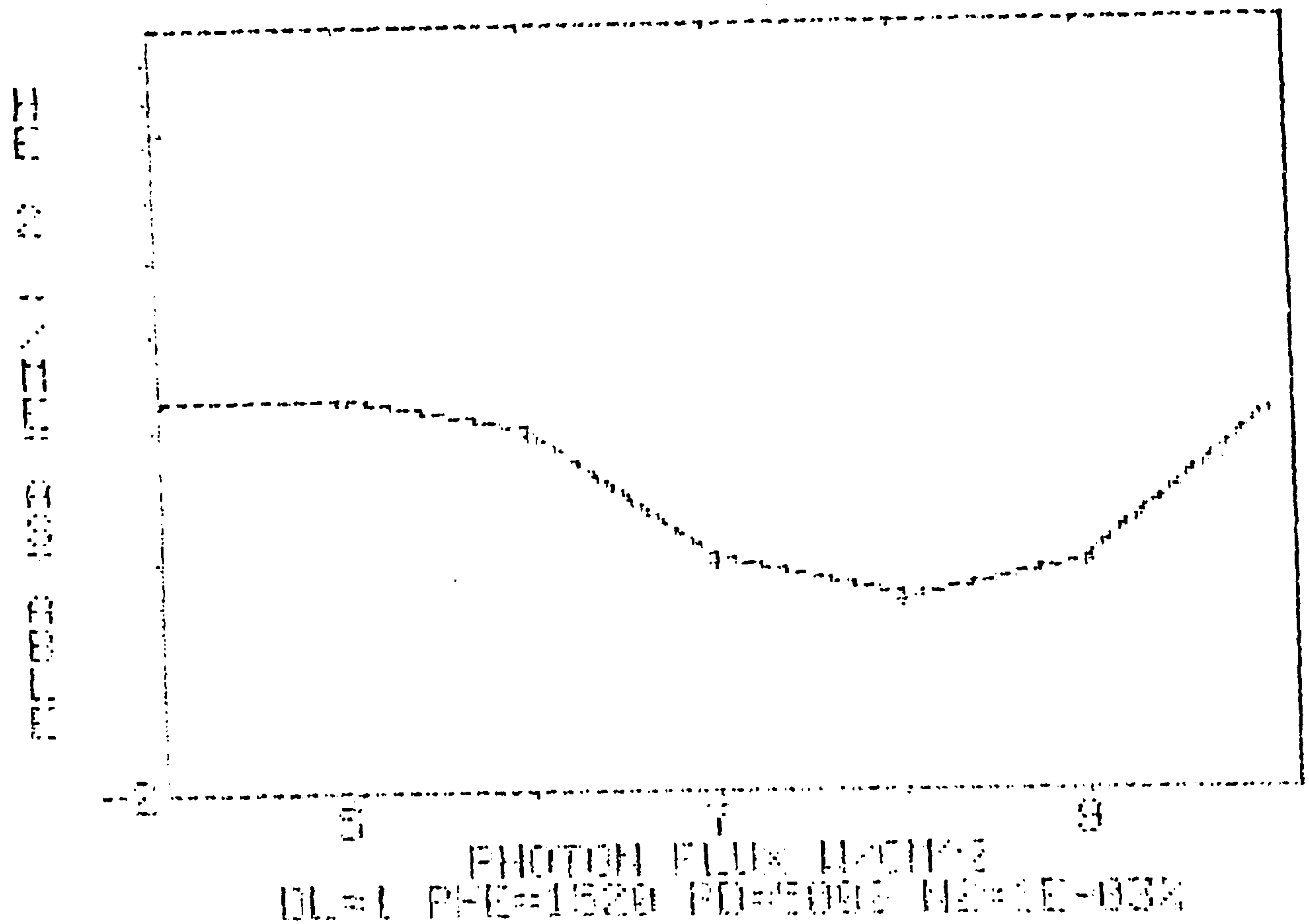

-2
5
7
9
PHOTON FLUX W/CM^2

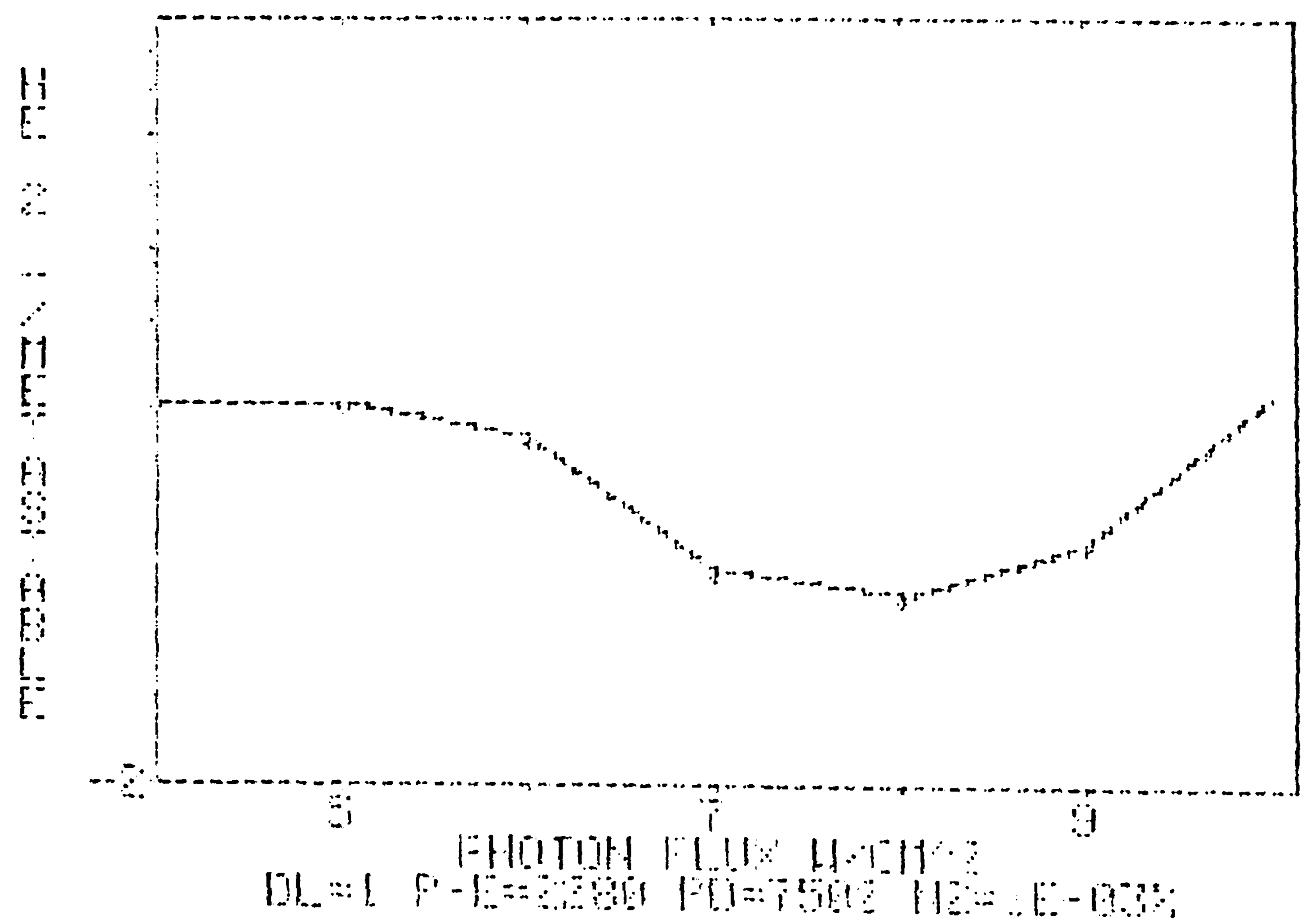
-2
5
7
9
PHOTON FLUX W/CM^2
DL=1 P-E=2280 PO=7502 H2=.E-003%

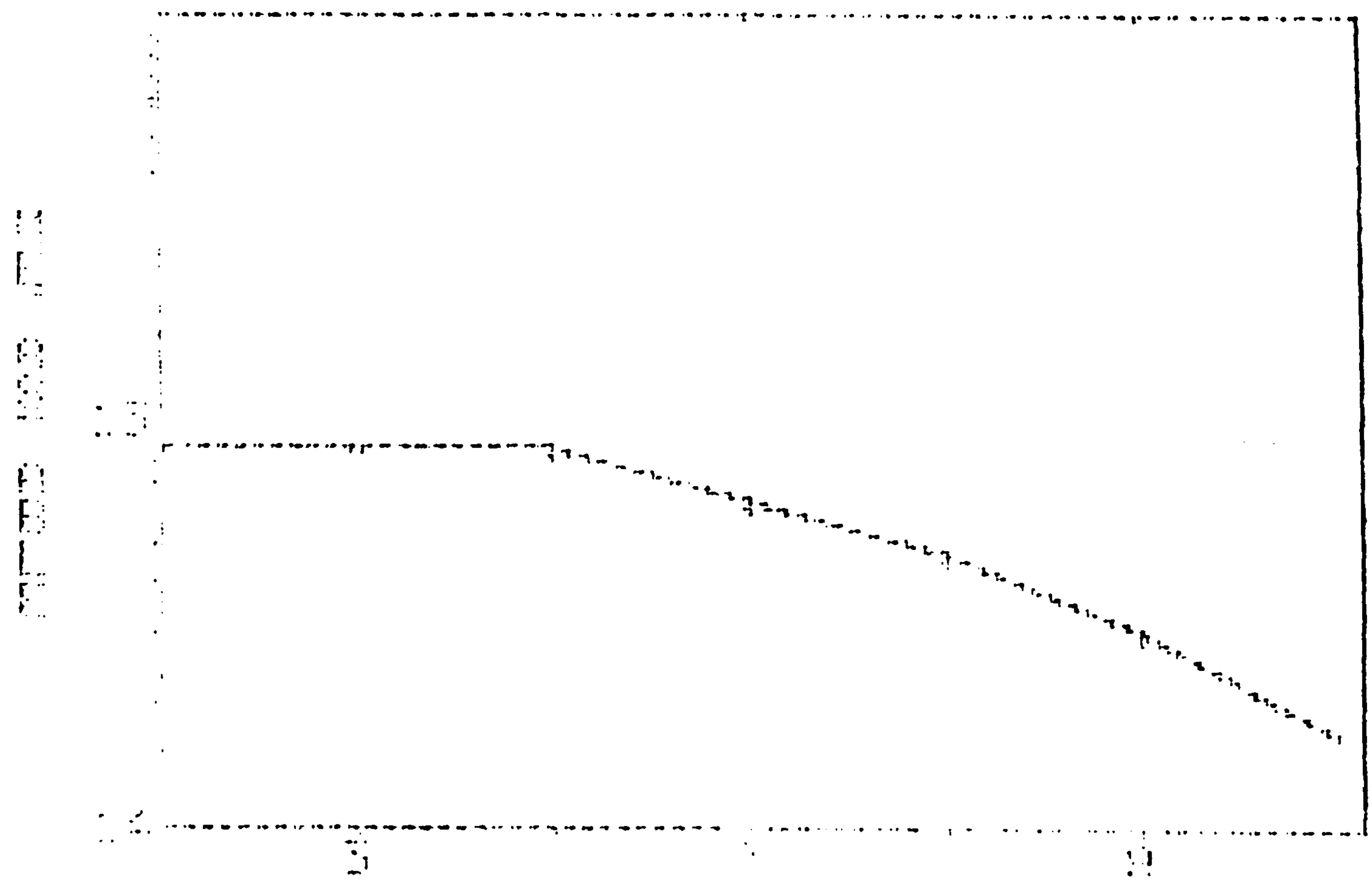

PHOTON FLUX (/CM 2

DL=1 PHE=3240 FD=10000 HZ=1E-03

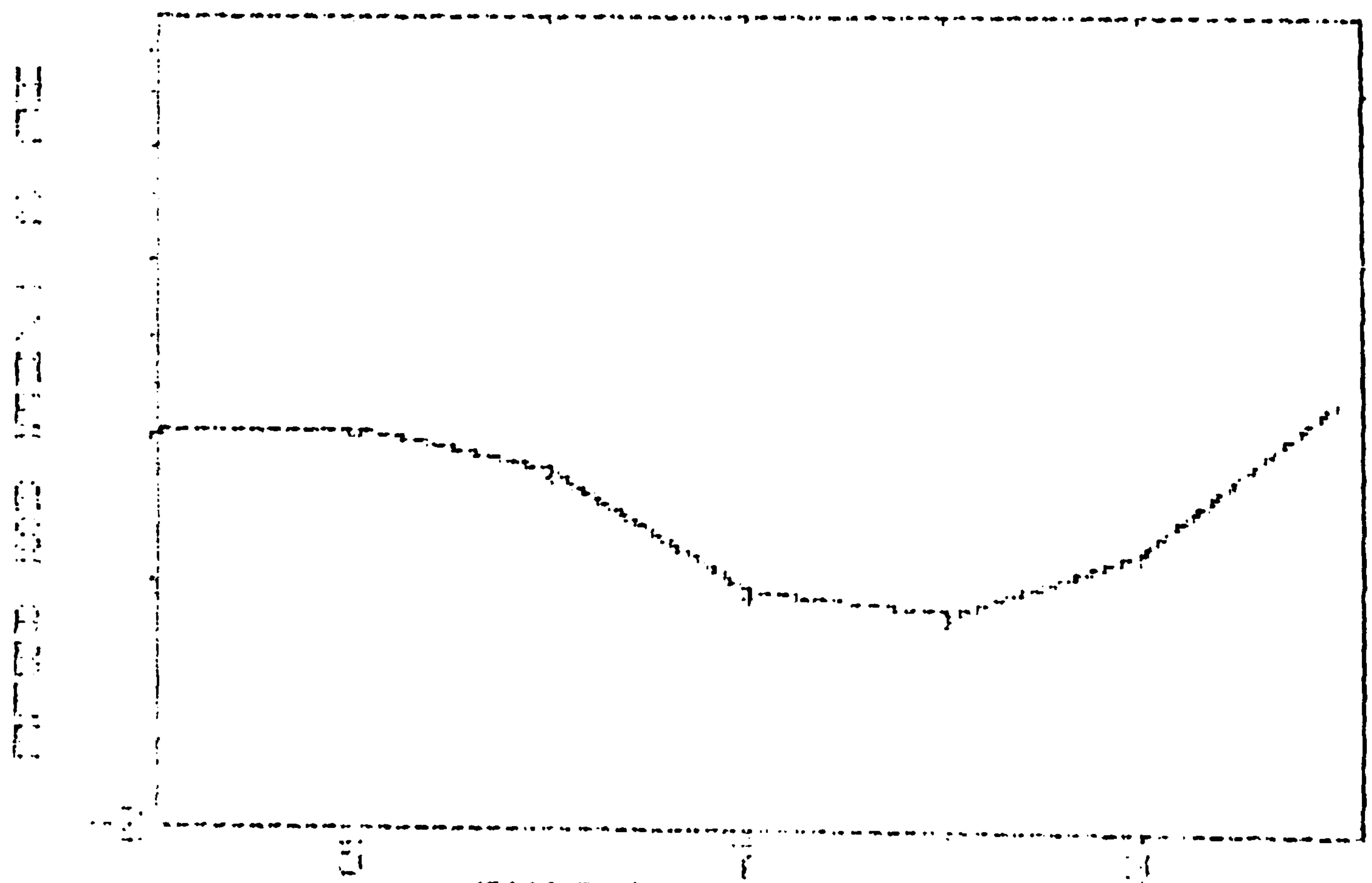

PHOTON FLUX W/CM^2
DL=1 PHE=3240 PD=10000 HZ=1E-03%

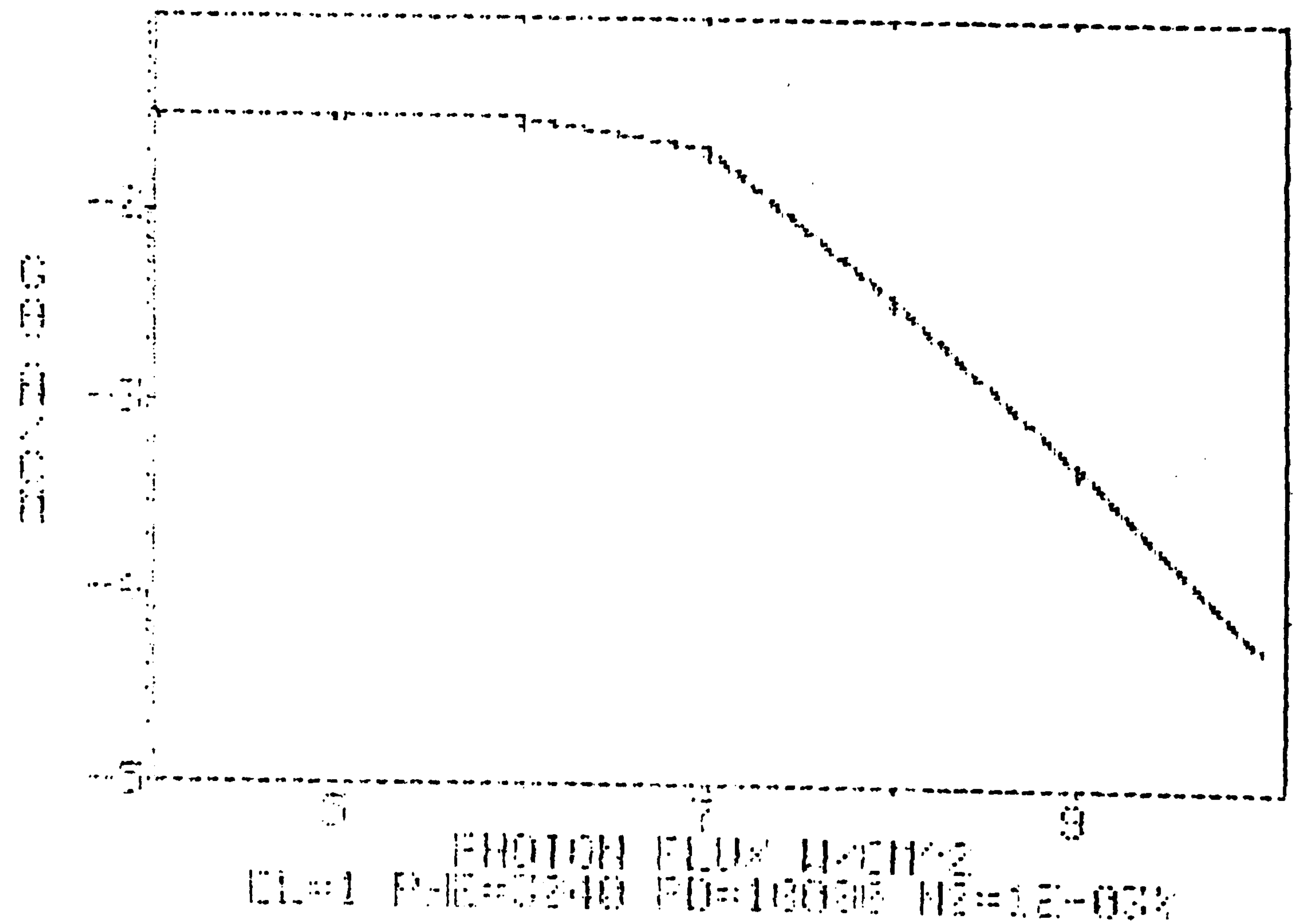
-2
-3
-4
-5
5
7
9
PHOTON FLUX W/CM^2
CL=1 P-E=3240 P0=10000 N2=1E-03%

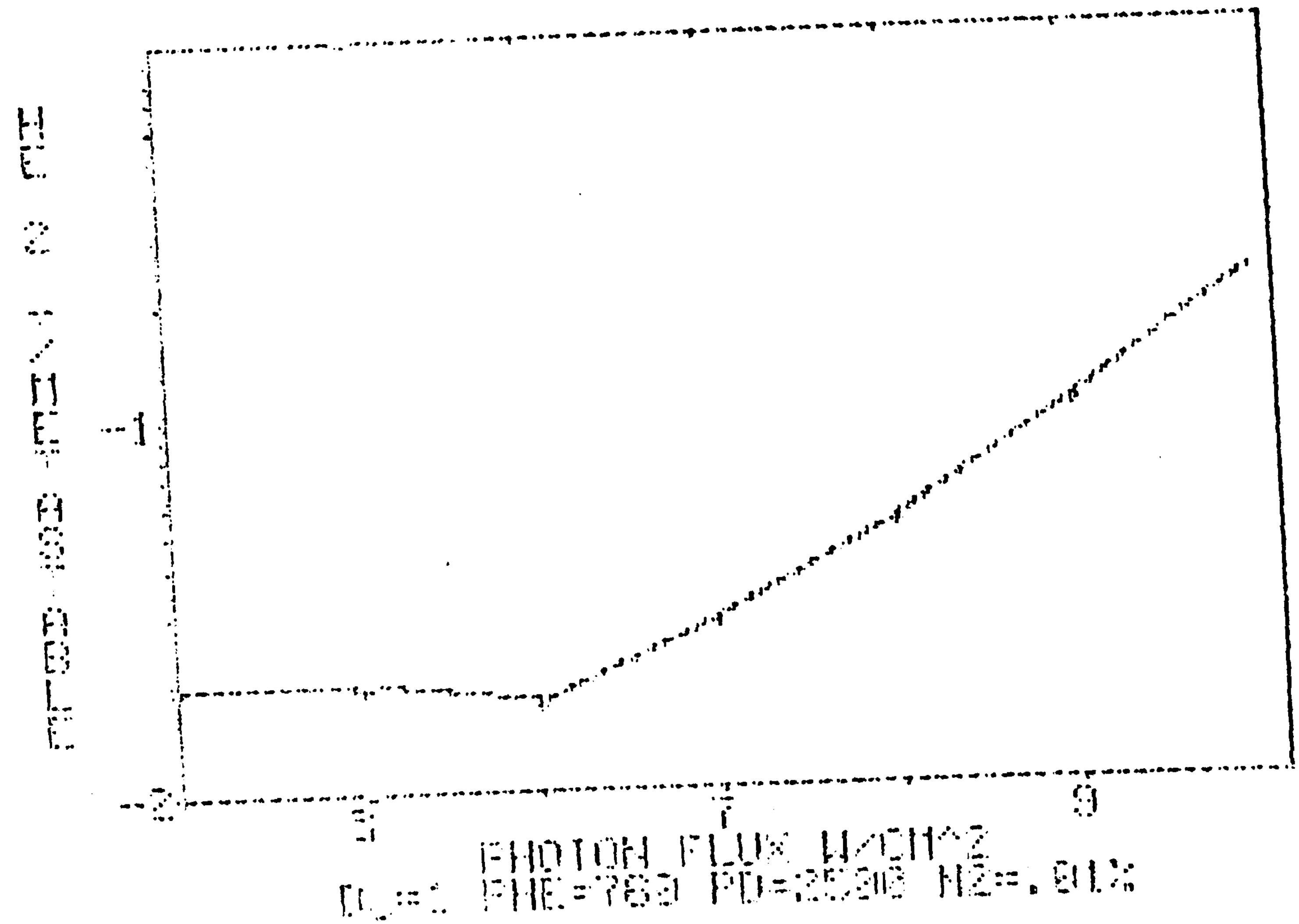
-1
-2
9
PHOTON FLUX W/CM^2

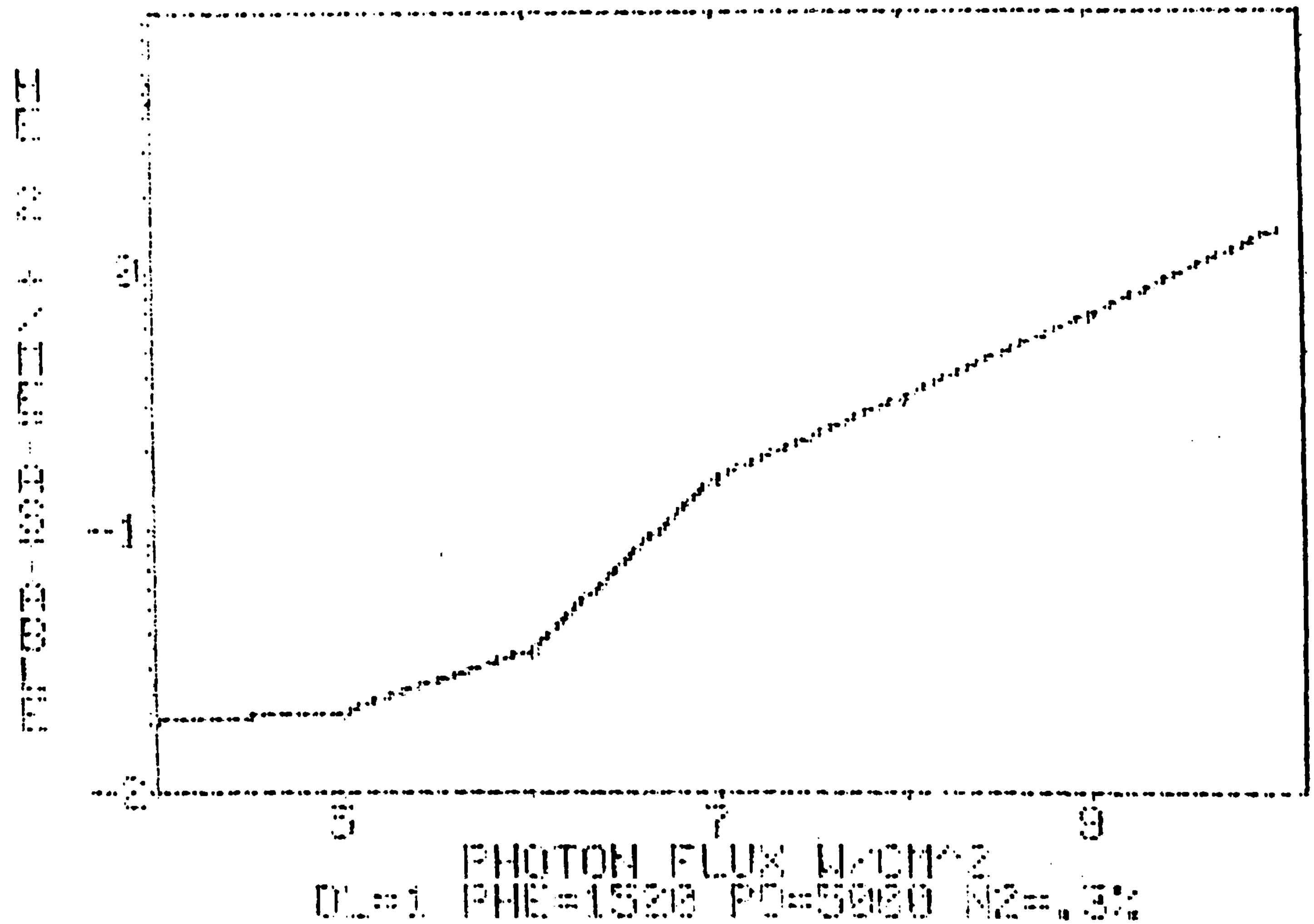

-1
-2
5
7
9
PHOTON FLUX W/CM^2
OL=1 PHE=1520 PO=5000 N2=.3%

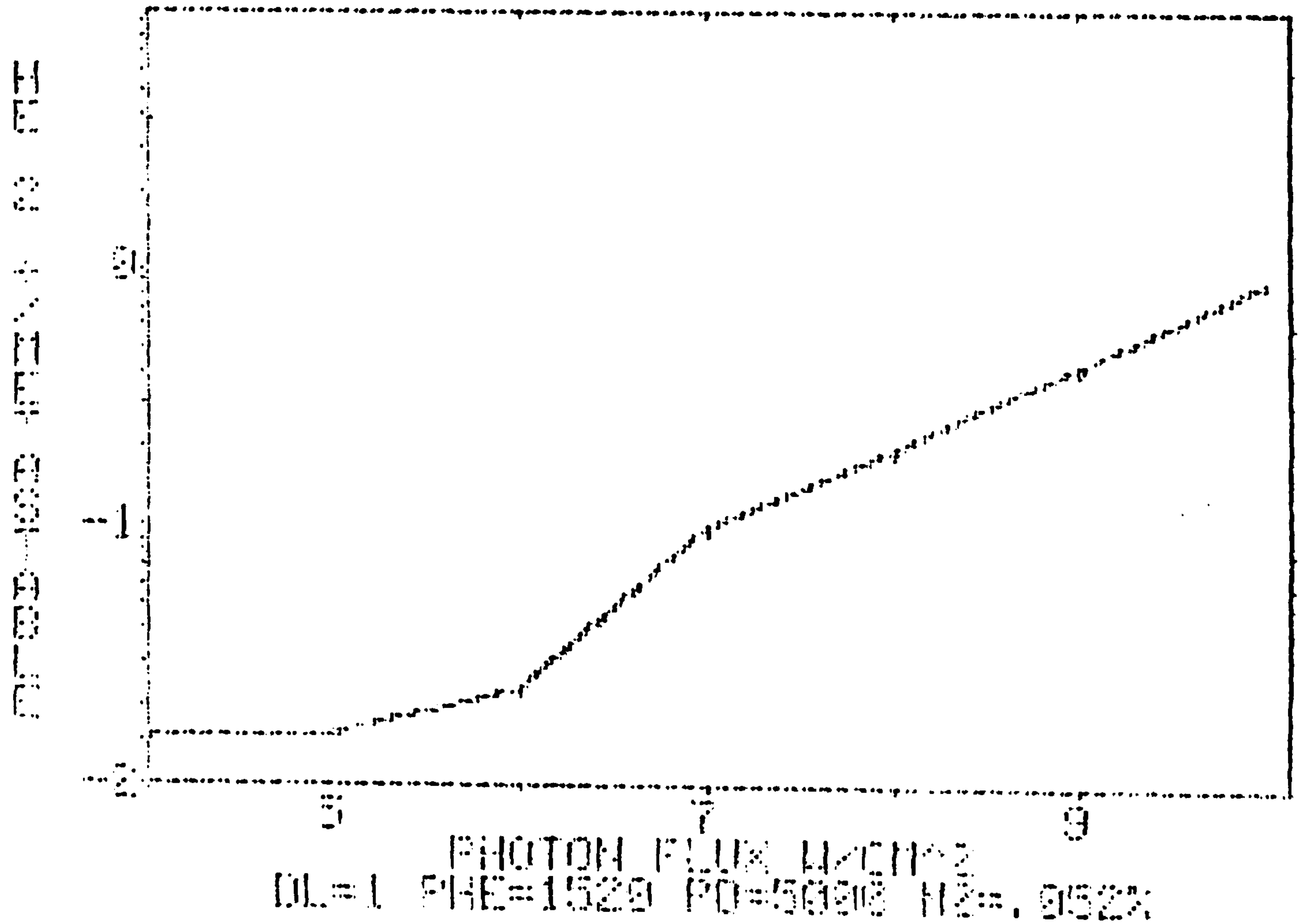
0
-1
-2
5
7
9
PHOTON FLUX W/CM^2
DL=1 PHE=1520 PO=5000 H2=.052%

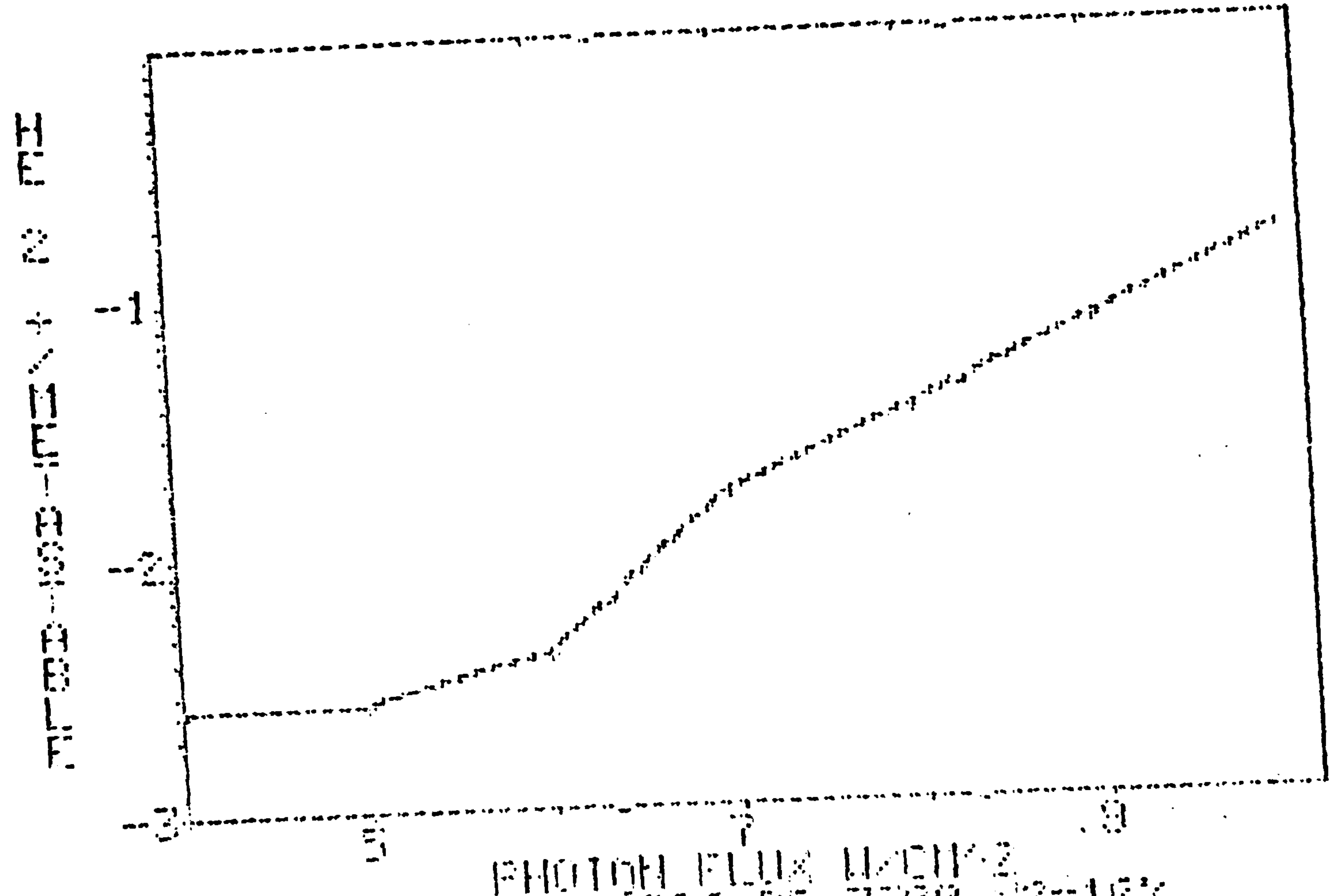

DL=1 PHE=2200 PO=7500 N2=10%

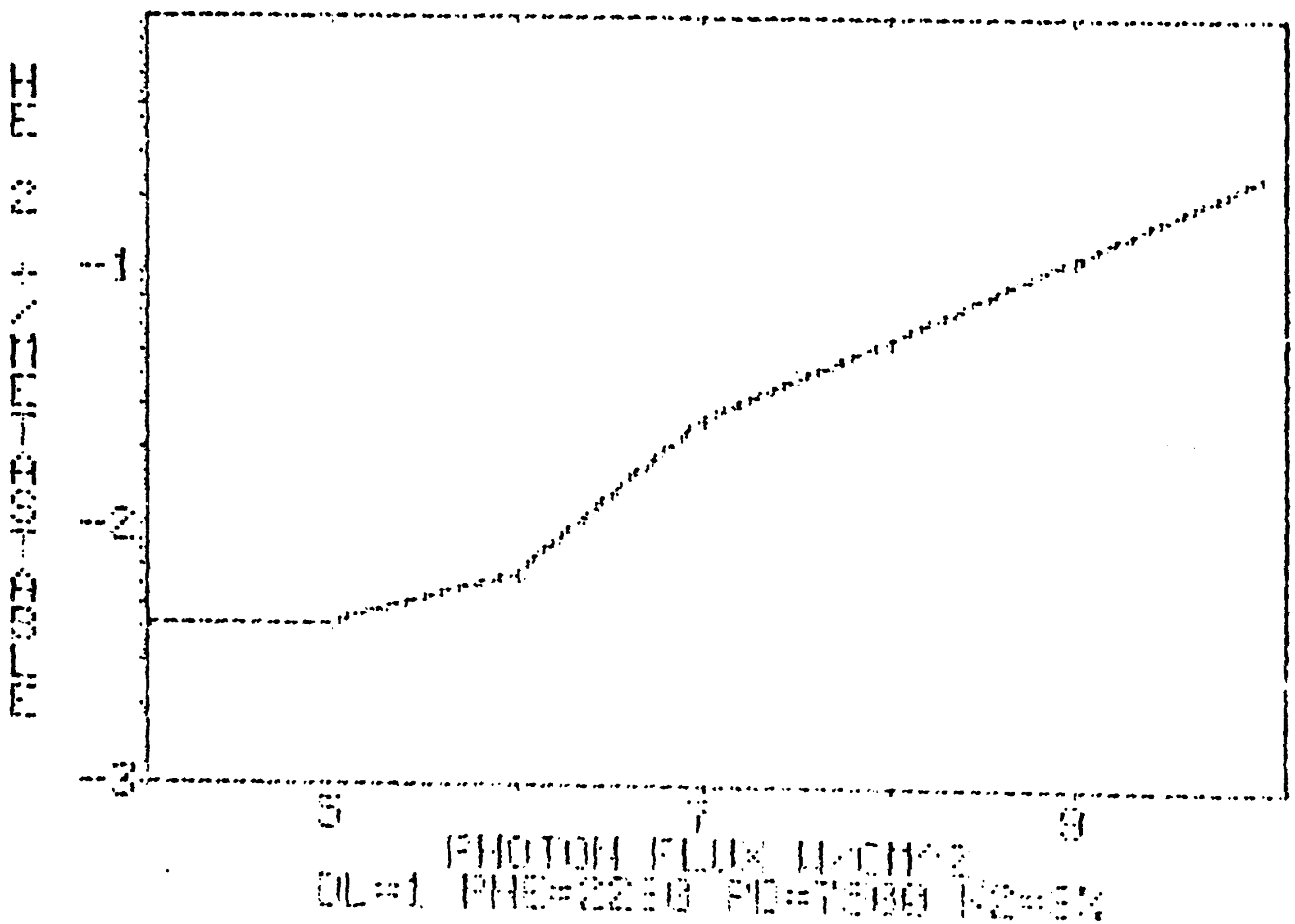
HE 2 +/METASTABLE
-1
-2
-3
5
7
9
PHOTON FLUX W/CM^2
DL=1 PHE=2210 PD=T300 N2=5%

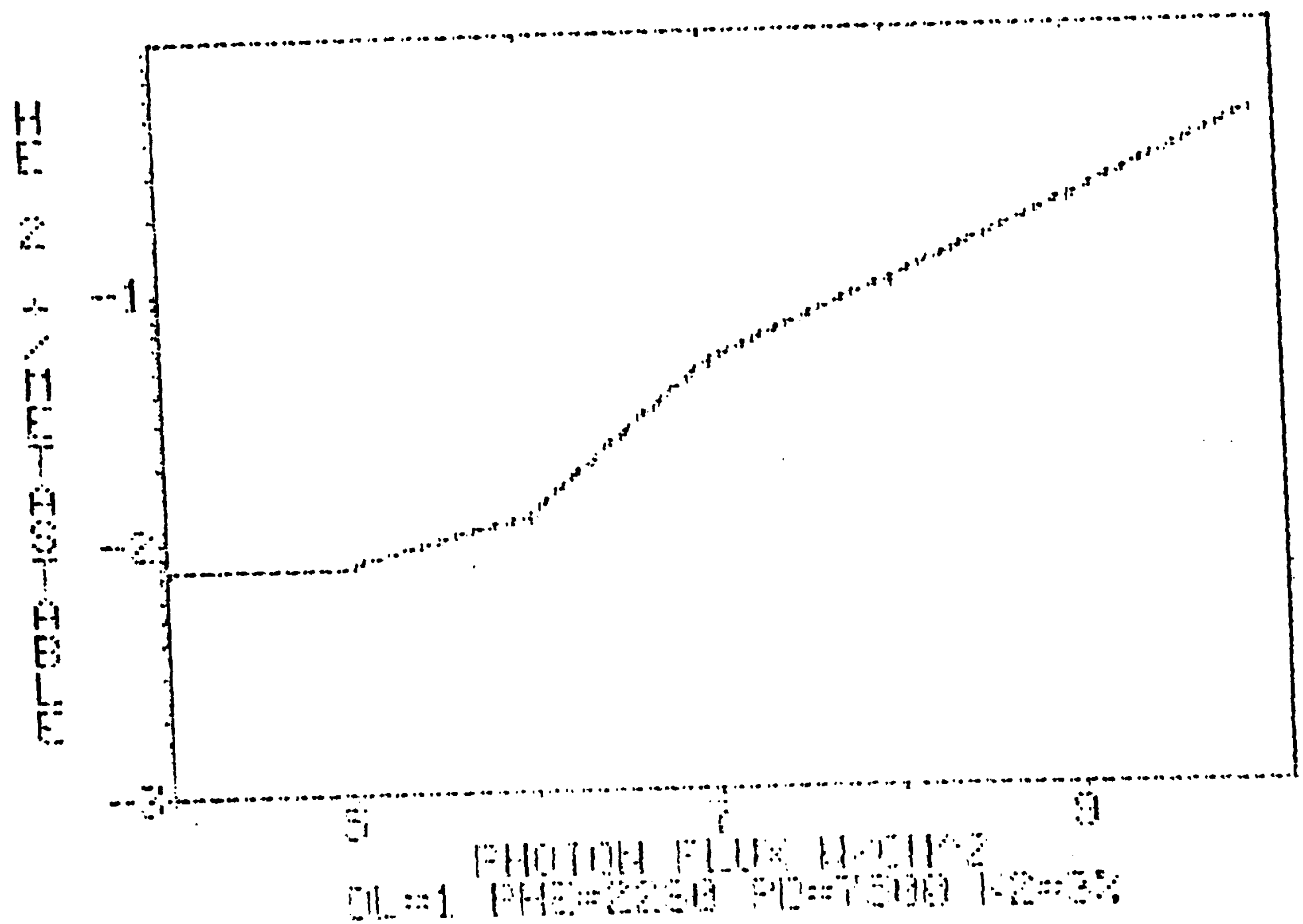
HE 2 + /METASTABLE
-1
-2
-3
5
7
9
PHOTON FLUX W/CM^2
OL=1 PHE=2250 PD=7500 N2=3%

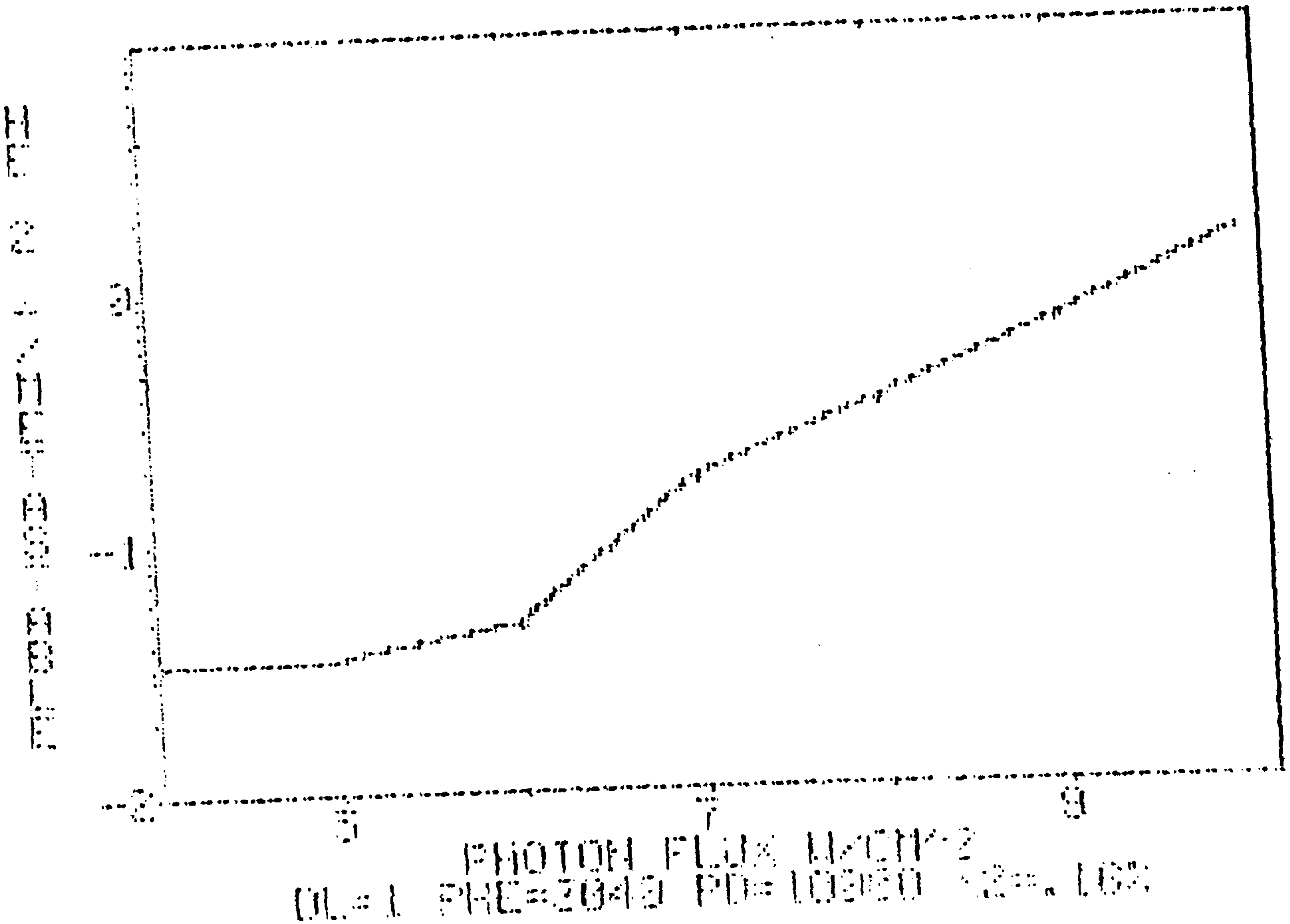

-2
-1
0
5
7
9
PHOTON FLUX W/CM^2

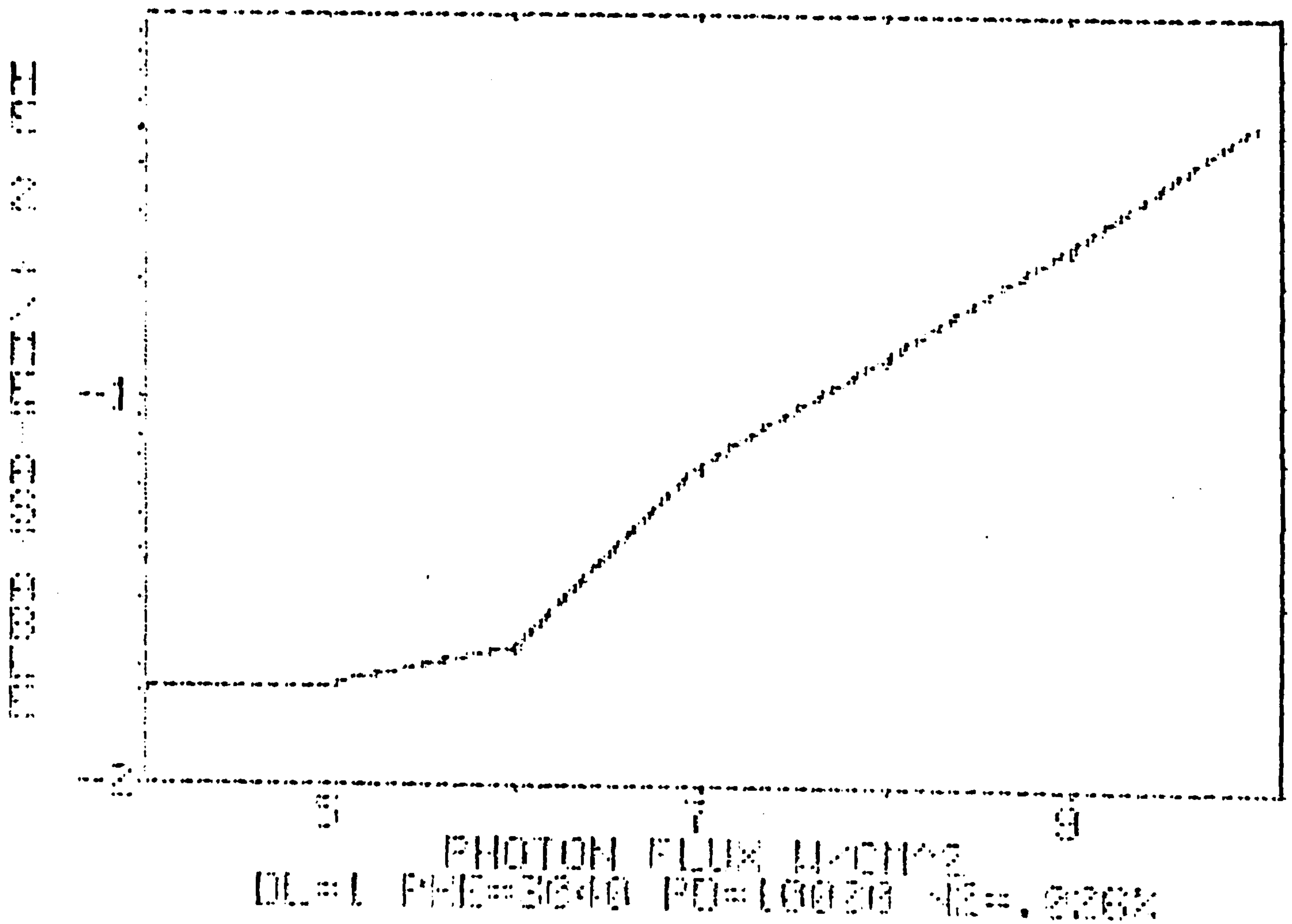
-1
-2
5
7
9
PHOTON FLUX W/CM^2

.1% N_2

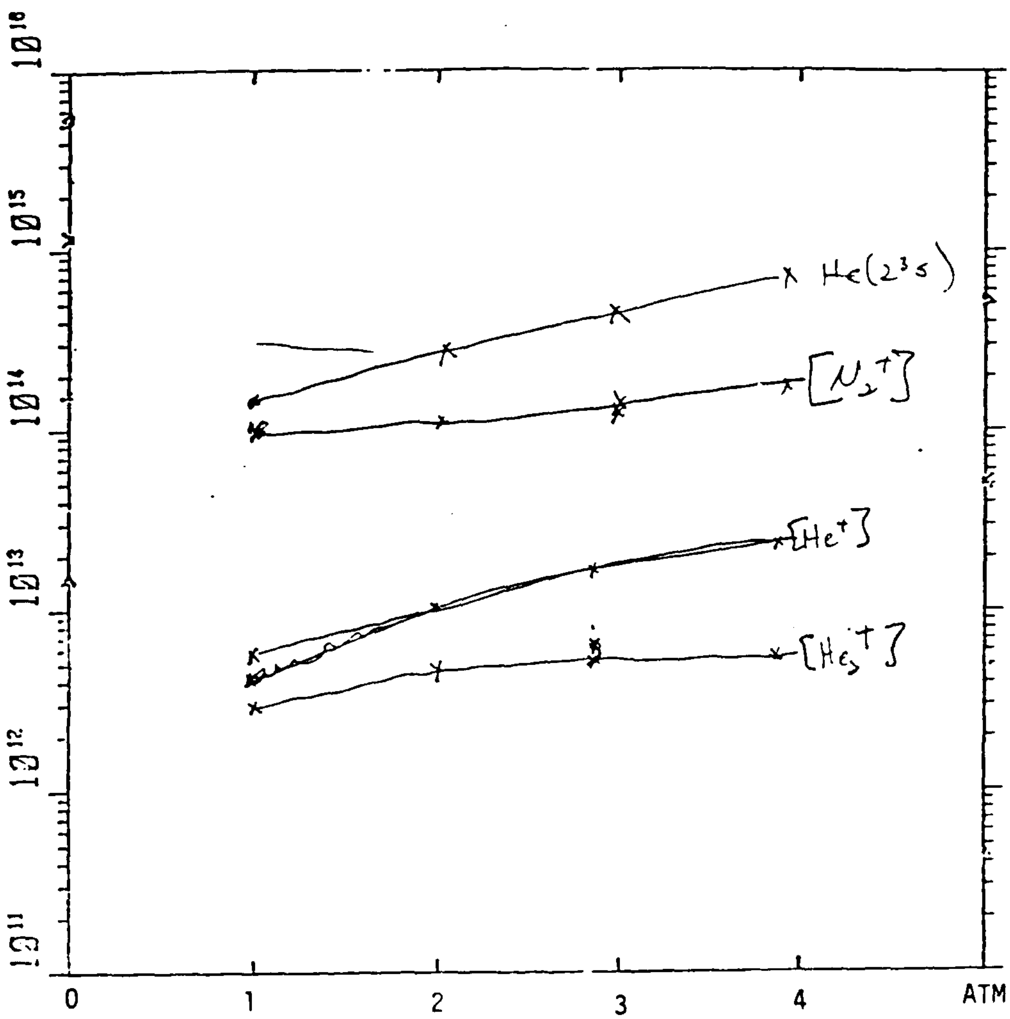

Power deposition 2.5 KW/cm^3 (5) (7.5) 10 KW/cm^3

APPENDIX II

RATE EQUATIONS FOR He-N_2 SYSTEM

1. $$\frac{d[He^+]}{dt} = S + \frac{\beta}{2}[He(2^3S)]^2 - k_1[N_2][He^+] - k_2 p_{He}^2 [He^+]$$

S - ENERGY DEPOSITED/SEC/CM^3 / W VALUE (ENERGY EXPENDED FOR 1 ION)

$\beta \rightarrow He(2^3S) + He(2^3S) \rightarrow He^+ + He + e$ METASTABLE-METASTABLE IONIZATION

$k_1 \rightarrow N_2 + He^+ \rightarrow N_2^+ + He$ CHARGE EXCHANGE

$k_2 \rightarrow 2\ He + He^+ \rightarrow He_2^+ + He$ THREE-BODY CONVERSION

2. $$\frac{d[He_2^+]}{dt} = k_2 p_{He}^2 [He^+] - .7\alpha[He_2^+][e] - k_{30}[N_2][He_2^+] - k_{31}[N_2][He_2^+][He]$$

$k_2 \rightarrow 2\ He + He^+ \rightarrow He_2^+ + He$ THREE-BODY CONVERSION

$\alpha \rightarrow He_2^+ + e + X \rightarrow$ COLLISIONAL RADIATIVE RECOMBINATION

$k_{30} \rightarrow N_2 + He_2^+ \rightarrow N_2^+ + 2\ He$ 2-BODY CHARGE TRANSFER

$k_{31} \rightarrow N_2 + He_2^+ \rightarrow N_2^+ + 2\ He + He$ 3-BODY CHARGE TRANSFER

3. $$\frac{d[He(2^3S)]}{dt} = S_m + 0.7\,\alpha[He_2^+][e] - \beta[He(2^3S)]^2 - \langle\sigma' v\rangle[N_2][He(2^3S)]$$

$$- A'[N_2][He(2^3S)] - 0.6p_{He}^2[He(2^3S)] - k_{40}[N_2][He(2^3S)]$$

$$- k_{41}[N_2][He(2^3S)][He] - k_5[He(2^3S)][e]$$

$S_m \Rightarrow S/0.56$

$\alpha \Rightarrow He_2^+ + e \rightarrow CRR \rightarrow He(2^3S)$ (70%)

$\beta \Rightarrow He(2^3S) + He(2^3S) \rightarrow He^+ + He + e$ METASTABLE-METASTABLE IONIZATION

$k_{40} \Rightarrow N_2 + He(2^3S) \rightarrow N_2^+ + He + e$ TWO-BODY PENNING IONIZATION

$k_{41} \Rightarrow N_2 + He(2^3S) + He \rightarrow N_2^+ + 2He + e$ THREE-BODY PENNING IONIZATION

$k_5 \Rightarrow He(2^3S) + e \rightarrow He + e$ (20 ev) SUPERELASTIC COLLISION

$\sigma' \Rightarrow \sigma_{weak}\rho$ WEAK FIELD DIPOLE-QUADRUPOLE INTERACTION

$A' \Rightarrow$ EINSTEIN COEFFICIENT SPONTANEOUS PHOTON EMISSION

$0.6p_{He}^2 \Rightarrow He(2^3S) + 2\,He \rightarrow He_2(2^3\Sigma)$ THREE-BODY CONVERSION TO MOLECULAR METASTABLE

4. $$\frac{d[N_2^+]}{dt} = k_1'[He^+][N_2] + k_{30}[He_2^+][N_2] + k_{31}[He_2^+][N_2][He]$$

$$+ k_{40}[He(2^3S)][N_2] + k_{41}[He(2^3S)][N_2][He]$$

$$+ \langle\sigma'v\rangle[He(2^3S)][N_2] + A'[He(2^3S)][N_2] - \alpha_{N_2}[e][N_2^+]$$

$k_1' \Rightarrow He^+ + N_2 \rightarrow He + N_2^+$ CHARGE EXCHANGE

$k_{30} \Rightarrow He_2^+ + N_2 \rightarrow 2He + N_2^+$ TWO-BODY CHARGE TRANSFER

$k_{31} \Rightarrow He_2^+ + N_2 + He \rightarrow 2He + He + N_2^+$ THREE-BODY CHARGE TRANSFER

$k_{40} \Rightarrow He(2^3S) + N_2 \rightarrow He + N_2^+ + e$ TWO-BODY PENNING IONIZATION

$k_{41} \Rightarrow He(2^3S) + N_2 + He \rightarrow 2He + N_2^+ + e$ THREE-BODY PENNING IONIZATION

$\alpha_{N_2} \Rightarrow N_2^+ + e \rightarrow N_2^*$ DISSOCIATIVE RECOMBINATION

5. $[e] = [He^+] + [He_2^+] + [N_2^+]$

February 1983

REPORTS DISTRIBUTION LIST FOR ONR PHYSICS DIVISION OFFICE
UNCLASSIFIED CONTRACTS

Director Defense Advanced Research Projects Agency Attn: Technical Library 1400 Wilson Blvd. Arlington, Virginia 22209	3 copies
Office of Naval Research Physics Division Office (Code 412) 800 North Quincy Street Arlington, Virginia 22217	3 copies
Office of Naval Research Director, Technology (Code 200) 800 North Quincy Street Arlington, Virginia 22217	1 copy
Naval Research Laboratory Department of the Navy Attn: Technical Library Washington, DC 20375	3 copies
Office of the Director of Defense Research and Engineering Information Office Library Branch The Pentagon Washington, DC 20301	3 copies
U.S. Army Research Office Box 1211 Research Triangle Park North Carolina 27709	2 copies
Defense Technical Information Center Cameron Station Alexandria, Virginia 22314	12 copies
Director, National Bureau of Standards Attn: Technical Library Washington, DC 20234	1 copy
Commanding Officer Office of Naval Research Western Detachment Office 1030 East Green Street Pasadena, California 91101	3 copies
Commanding Officer Office of Naval Research Eastern/Central Detachment Office 495 Summer Street Boston, Massachusetts 02210	3 copies

Commandant of the Marine Corps | 1 copy
Scientific Advisor (Code RD-1)
Washington, DC 20380

Naval Ordnance Station | 1 copy
Technical Library
Indian Head, Maryland 20640

Naval Postgraduate School | 1 copy
Technical Library (Code 0212)
Monterey, California 93940

Naval Missile Center | 1 copy
Technical Library (Code 5632.2)
Point Mugu, California 93010

Naval Ordnance Station | 1 copy
Technical Library
Louisville, Kentucky 40214

Commanding Officer | 1 copy
Naval Ocean Research & Development Activity
Technical Library
NSTL Station, Mississippi 39529

Naval Explosive Ordnance Disposal Facility | 1 copy
Technical Library
Indian Head, Maryland 20640

Naval Ocean Systems Center | 1 copy
Technical Library
San Diego, California 92152

Naval Surface Weapons Center | 1 copy
Technical Library
Silver Spring, Maryland 20910

Naval Ship Research and Development Center | 1 copy
Central Library (Code L42 and L43)
Bethesda, Maryland 20084

Naval Avionics Facility | 1 copy
Technical Library
Indianapolis, Indiana 46218

DISTRIBUTION LIST

(as specified in contract)

COPY # ISSUED	ADDRESSEE	# OF COPIES ISSUED
# 1	Scientific Officer Director Mathematical & Physical Sciences Division OFFICE OF NAVAL RESEARCH 800 North Quincy Street Arlington, VA 22217 ATTN: Dr. B. R. Junker REF: Contract Number N00014-82-C-0071	1 copy (include Form DD250)
# 2	OFFICE OF NAVAL RESEARCH 800 North Quincy Street Arlington, VA 22217 ATTN: David K. Beck Contracting Officer	1 copy
#48-53	NAVAL RESEARCH LABORATORY ATTN: Code 2627 Washington, D.C. 20375	6 copies
#18-29	DEFENSE TECHNICAL INFORMATION CENTER Building 5, Cameron Station Alexandria, VA 22314	12 copies (include Form DD1473)
# 3	OFFICE OF NAVAL RESEARCH Western Regional Office 1030 East Green Street Pasadena, CA 91106 ATTN: Dr. Robert Behringer	1 copy

ILMED

– 8